LIBSCUFF Implementation and Technical Details

Homer Reid

October 11, 2011

Contents

1 Geometries in LIBSCUFF

LIBSCUFF thinks of a geometry as consisting of a collection of three-dimensional *regions*, bounded by two-dimensional *surfaces.*

Each region $\mathcal{R}^r$ is a contiguous volume throughout which the permittivity and permeability are spatially constant,

$$\epsilon(\mathbf{x},\omega) \equiv \epsilon^r(\omega), \qquad \mu(\mathbf{x},\omega) \equiv \mu^r(\omega)$$

where $\epsilon^r(\omega)$ and $\mu^r(\omega)$ may be arbitrary user-specified functions of frequency. (Only linear, isotropic ϵ and μ are supported.) The region with index $r = 0$ is known as the "exterior" medium of the LIBSCUFF geometry; it is always present in every LIBSCUFF geometry and has by default the permittivity and permeability of vacuum. The user may redefine the material properties of the exterior medium as desired.

Each surface is described by a surface mesh consisting of a union of flat triangular panels. Each surface lies at the interface between precisely two regions. We identify one of these two regions as the "exterior" region for the surface in question, and the other region is the "interior." The normal vector to the surface is always defined to point into the "exterior" region.[1] (This is true even for open surfaces; in this case the terminology "exterior" and "interior" doesn't quite make sense, but we can certainly still pick one of the two regions between which a surface lies and decide that the normal vector will point into that region, and we call that region the "exterior" region for the open surface.)

The regions and surfaces that define LIBSCUFF geometries are specified in *geometry files,* conventionally given the file extension `.scuffgeo`. The `.scuffgeo` file is parsed to create an instance of a `C++` class named `RWGGeometry`. This is a big class containing lots of data fields and methods, but for the purposes of this section the most important fields are the following:

-2-4pt-2-4pt

```
class RWGGeometry
 {
    int NumRegions;
    char **RegionLabels;

    int NumSurfaces;
    RWGSurface **Surfaces;
 };
```

Simple geometries: `OBJECT` specifications

The simplest type of LIBSCUFF geometry consists of one or more compact homogeneous objects embedded in an external medium. In this case, each object is described by a *closed* surface mesh (specified to LIBSCUFF as a mesh file in

[1] This requires that surfaces be *orientable*; Klein bottles are thus explicitly forbidden in LIBSCUFF geometries, although PEC Möbius strips are allowed.

one of the supported mesh file formats) together with an material designation. Here's an example:

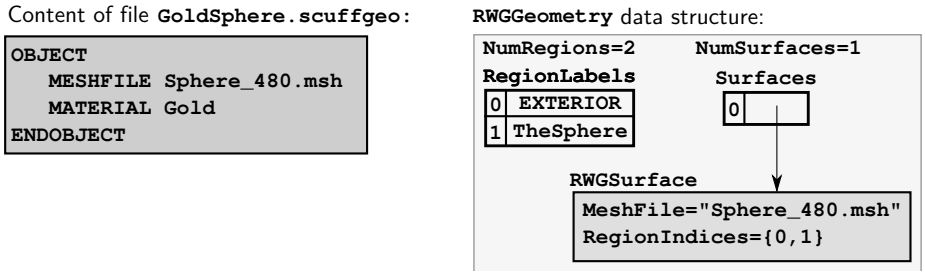

Figure 1: A simple `.scuffgeo` file and some fields in the corresponding `RWGGeometry` structure.

In the language of regions and surfaces discussed above, each `OBJECT` statement adds one new region and one new surface to a geometry. The newly added region is always taken to be the interior region associated with the newly added surface, and corresponds to the volume inside the object; the new surface exists at the interface between this region and the exterior medium.

We said above that surface meshes for compact objects should be *closed* surfaces. The exception to this statement is that PEC (perfectly electrically conducting) or IPEC (imperfectly electrically conducting) bodies may be described by open surfaces. (An IPEC body is a PEC body with finite surface conductivity). For both PEC and IPEC bodies the interior fields vanish identically, and there is no need for such bodies to have finite interior volume. An `OBJECT` statement declaring a new PEC or IPEC object adds one new surface but *not* one new region to the geometry.

Simple geometries: Nested objects

It is possible for an object defined by an `OBJECT` declaration to be fully contained inside another `OBJECT`. The nesting inclusion relationship is automatically detected by LIBSCUFF.

More complicated geometries: `REGION` and `SURFACE` statements

Some geometries are too complicated to be defined as collections of compact objects bounded by closed surfaces. One example is a composite sphere in which the upper and lower hemispheres consist of different materials. Another example is a metallic nanoparticle (say, a disc) lying atop a dielectric substrate. The common feature of these two examples that prevents description in terms of simple closed objects is the presence of *multi-material junctions*; these are

one-dimensional subspaces at which three or more material regions meet. For the composite sphere, the multi-material junction would be the equator; for the disc on the substrate, it would be the lower circumference of the disc.

Geometries like this are described in LIBSCUFF using `REGION` and `SURFACE` statements. For example, the composite sphere above may be specified like this:

Content of file **`BiHemisphere.scuffgeo`**:

```
REGION Exterior        MATERIAL VACUUM
REGION UpperHemisphere MATERIAL Gold
REGION LowerHemisphere MATERIAL Silicon

SURFACE UpperHemisphereSurface
 MESHFILE UpperHemisphere.msh
 REGIONS  Exterior UpperHemisphere
ENDSURFACE

SURFACE LowerHemisphereSurface
 MESHFILE LowerHemisphere.msh
 REGIONS  Exterior LowerHemisphere
ENDSURFACE

SURFACE EquatorialPlane
 MESHFILE EquatorialPlane.msh
 REGIONS  UpperHemisphere LowerHemisphere
ENDSURFACE
```

`RWGGeometry` data structure:

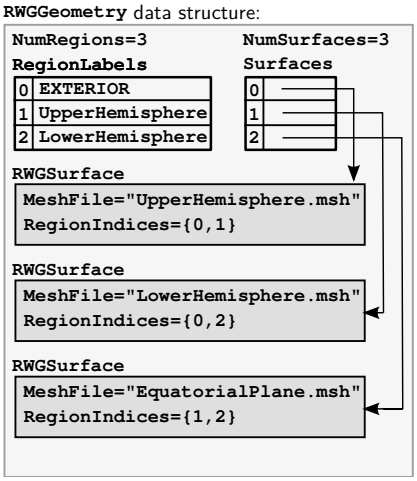

Figure 2: A more complex `.scuffgeo` file and some fields in the corresponding `RWGGeometry` structure.

Extended geometries: `LATTICE` statements

Extended geometries are described using `LATTICE` statements in the `scuffgeo` file. For example, here's an infinite square-lattice array of gold spheres:

```
          LATTICE
                  VECTOR 1 0
                  VECTOR 0 1
          ENDLATTICE
-2-4pt-2-4pt
          OBJECT TheSphere
                  MESHFILE Sphere_480.msh
                  MATERIAL Gold
          ENDOBJECT
```

It is also possible for surfaces to straddle the lattice-cell boundaries. This will be the case, for example, if you are describing an infinite planar surface (possibly with holes). In this case, the surface mesh must be *compatible* with the lattice specification, in the sense that every triangle edge that lies on the unit-cell boundary must have an image edge lying one lattice-translate away.

Extended geometries in which the exterior medium is non-contiguous

In some extended geometries, it may be possible for the exterior medium to be non-contiguous. For example, consider a thin film described by two planar surfaces (the upper and lower surfaces of the film) with a `LATTICE` statement indicating the surfaces are infinitely extended (comprised of an infinite 2D lattice of the unit-cell surfaces). In this case, you probably think of the region above the upper surface and the region below the lower surface as both belonging to the same region, but as far as LIBSCUFF is concerned they must be two different regions.

The reason for this is the following: Suppose both the upper half-space and the lower half-space were the same region (say `Exterior`). Then the upper and lower surfaces of the slab would both have `Exterior` as one of the two regions at whose interface they lie, and thus surface currents on both the upper and lower surfaces would contribute to the scattered fields at all points in `Exterior`. But this would be incorrect: Points in the upper half-space receive scattered-field contributions only from currents on the upper surface, while points in the lower half-space receive contributions only from the lower surface.

The situation would be different if the upper and lower half-spaces were *contiguous*—which would be the case, for example, if the thin-film slab had a hole in it. In this case, the upper and lower film surfaces (as well as the hole sidewall surfaces) all form part of a single bounding surface separating the film interior from `Exterior`, and hence surface currents on all of these surfaces contribute to the scattered fields at points in `Exterior`.

2 Representation of Surface Currents in LIBSCUFF

Surface Currents

LIBSCUFF is based on the surface-integral-equation approach to computational electromagnetism. In this approach, the fundamental unknowns are tangential *surface currents* flowing on the surfaces that lie at the interface between homogeneous material regions.

Electric and magnetic surface currents at dielectric interfaces

For the general case of a surface lying between two dielectric regions, we have both an electric surface-current distribution $\mathbf{K}(\mathbf{x})$ and a magnetic surface-current distribution $\mathbf{N}(\mathbf{x})$ (here $\mathbf{x}$ is a point lying on the surface). Both $\mathbf{K}$ and $\mathbf{N}$ are strictly *tangential* to the surface; they have no normal component.

Physical interpretation of surface currents

One way to interpret the $\mathbf{K}$ and $\mathbf{N}$ currents is as effective source distributions confined to the surfaces. In a real scattering problem involving dielectric bodies, the incident fields induce a physical volume electric current distribution $\mathbf{J}(\mathbf{r})$ which is nonzero for all points $\mathbf{r}$ inside dielectric bodies, and the scattered fields are just the fields radiated by this source distribution. The surface currents $\mathbf{K}$ and $\mathbf{N}$ are *fictitious* or ("effective") source distributions with the property that the fields they radiate exactly reproduce the field radiated by the physical source distribution $\mathbf{J}$, both inside and outside the body. What is unphysical about $\mathbf{K}$ and $\mathbf{N}$ is that **(a)** they are confined to the surfaces, whereas the physical induced source distribution $\mathbf{J}$ exists throughout the volume, and **(b)** they include magnetic currents $\mathbf{N}$, i.e. moving magnetic monopoles, which do not actually exist in our universe.[2] However, the fields radiated by $\mathbf{K}$ and $\mathbf{N}$ are perfectly physical.

Another, perhaps more direct, way to interpret the $\mathbf{K}$ and $\mathbf{N}$ currents is that they are nothing but rotated versions of the tangential components of the total electric and magnetic fields at the surface, i.e. we have

$$\mathbf{K}(\mathbf{x}) = \hat{\mathbf{n}} \times \mathbf{H}^{\rm tot}(\mathbf{x}), \qquad \mathbf{N}(\mathbf{x}) = -\hat{\mathbf{n}} \times \mathbf{E}^{\rm tot}(\mathbf{x}).$$

Electric surface currents on PEC surfaces

In the special case of a PEC surface—whether closed or open—the magnetic surface current vanishes identically ($\mathbf{N} = 0$) and only the electric surface current $\mathbf{K}$ is nonzero. In this case, the two interpretations of the surface currents discussed above coincide physically: Incident fields really do excite physical electric currents on the surfaces of PEC bodies, these currents really are strictly

[2] Perhaps we should say no more than *one* of them exists in our universe: `http://prl.aps.org/abstract/PRL/v48/i20/p1378_1`.

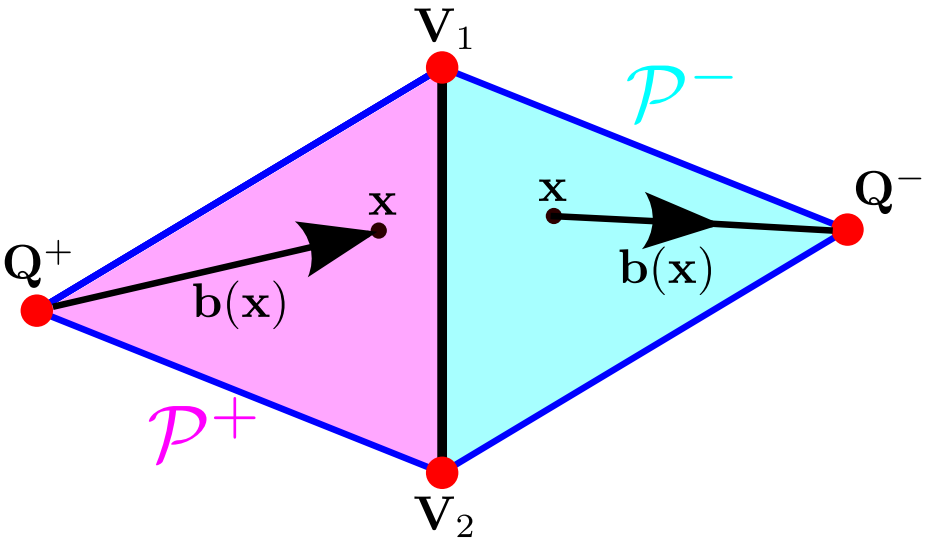

Figure 3: Notation for RWG basis functions.

confined to the surfaces (in the idealized limit of a *perfect* electric conductor), and the field radiated by these induced currents really is the full scattered field.

RWG Basis Functions

LIBSCUFF uses RWG basis functions[3] to describe electric and magnetic surface currents flowing on the surfaces in a geometry. Each RWG basis function is assigned to a single interior edge in a surface mesh discretization, and is nonvanishing only on the two triangular panels that share that edge.

To construct the RWG basis function associated with an edge (Figure 3), arbitrarily choose one of the two panels to be the *positive* panel $\mathcal{P}^+$ associated with the basis function, while the other panel is the *negative* panel $\mathcal{P}^-$. Let the vertices of the common edge be $\mathbf{V}_1$ and $\mathbf{V}_2$, and let the third vertex of $\mathcal{P}^+$ be the positive or *source* vertex $\mathbf{Q}^+$ for the basis function, while the other opposite vertex will be the negative or *sink* vertex $\mathbf{Q}^-$. Then the RWG basis function $\mathbf{b}(\mathbf{x})$ associated with the edge is defined as follows:

$$\mathbf{b}(\mathbf{x}) = \begin{cases} +\frac{l}{2A^+}(\mathbf{x}-\mathbf{Q}^+), & \mathbf{x}\in\mathcal{P}^+ \\ -\frac{l}{2A^+}(\mathbf{x}-\mathbf{Q}^-), & \mathbf{x}\in\mathcal{P}^- \\ 0, & \text{otherwise} \end{cases}$$

where l is the length of the common edge (the distance $\mathbf{V}_1\mathbf{V}_2$) and $\mathbf{A}^\pm$ are the areas of $\mathcal{P}^\pm$. Thus the RWG function describes a current that emanates from

[3] S. M. Rao, D. R. Wilton, A. W. Glisson, *IEEE Trans. Antennas Propagat.* **AP-30** 409 (1982).

$\mathbf{Q}^+$, grows linearly in strength as it flows along the surface of $\mathcal{P}^+$ toward the common edge, begins decreasing linearly in strength after crossing over that edge into $\mathcal{P}^-$, and is sunk into $\mathbf{Q}^-$. There is no current flow outside the pair of panels because $\mathbf{b}(\mathbf{x})$ has no component normal to any of the four exterior edges of the panel pair.

Figure 4 illustrates some of the LIBSCUFF data structures associated with a single RWG basis function embedded in a surface mesh.

Half-RWG Basis Functions

It is also possible to assign basis functions to *exterior* edges of surface meshes, i.e. edges that lie on the boundary of open surfaces. In contrast to interior edges, exterior edges are associated within only one panel, not two panels. SCUFF-EM adopts the convention that this panel is the positive panel $\mathcal{P}^+$ for the edge, while there is no negative panel $\mathcal{P}^-$. For exterior edges, the `iMPanel` field of the `RWGEdge` structure is set to `-1`.

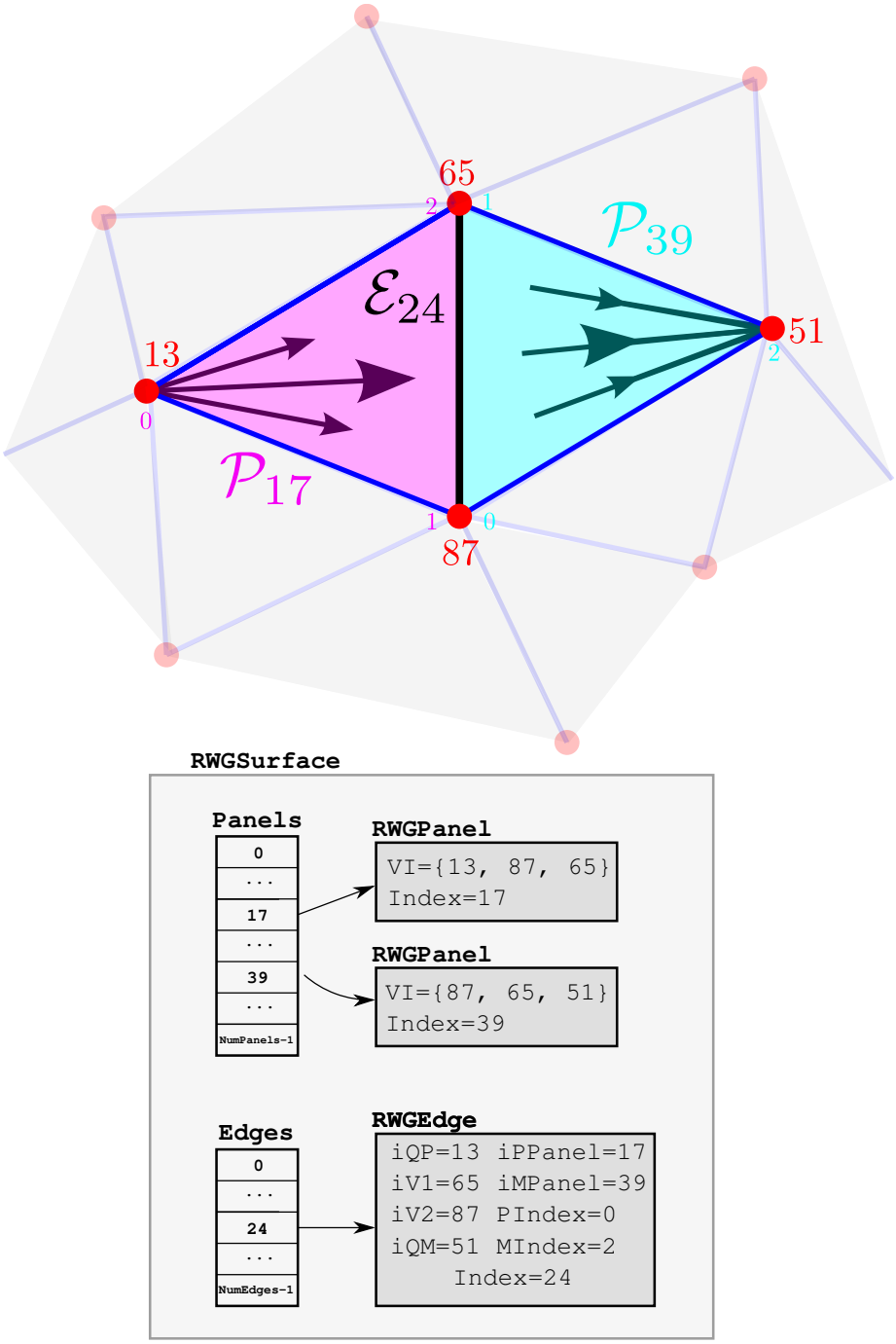

Figure 4: A single RWG basis function associated with an internal edge on an `RWGSurface`, and some portions of data structures within the corresponding `RWGSurface` instance that describe this basis function.

3 Homogeneous Dyadic Green's Functions

Before proceeding, we must pause briefly to establish our conventions and notation for homogeneous dyadic Green's functions.

Consider a spatial region characterized by spatially uniform relative permittivity and permeability ϵ^r and μ^r. If we have known distributions of electric and magnetic current $\mathbf{J}(\mathbf{x})$ and $\mathbf{M}(\mathbf{x})$, we can compute the electric and magnetic fields in terms of these currents and the properties of the medium, and the relevant convolution kernels in this procedure are the dyadic Green's functions (DGFs):

$$E_i(\mathbf{x},\omega) = \int \Big\{ \Gamma^{\rm EE}_{ij}(\epsilon^r,\mu^r;\omega;\mathbf{x},\mathbf{x}')J_j(\mathbf{x}') + \Gamma^{\rm EM}_{ij}(\epsilon^r,\mu^r;\omega;\mathbf{x},\mathbf{x}')M_j(\mathbf{x}') \Big\}\, d\mathbf{x}'$$

$$H_i(\mathbf{x},\omega) = \int \Big\{ \Gamma^{\rm ME}_{ij}(\epsilon^r,\mu^r;\omega;\mathbf{x},\mathbf{x}')J_j(\mathbf{x}') + \Gamma^{\rm MM}_{ij}(\epsilon^r,\mu^r;\omega;\mathbf{x},\mathbf{x}')M_j(\mathbf{x}') \Big\}\, d\mathbf{x}'.$$

Explicit expressions for the DGFs are

$$\mathbf{\Gamma}^{\rm EE}(\epsilon^r,\mu^r,\omega,\mathbf{x},\mathbf{x}') = iZ_0Z^r k^r\, \mathbf{G}(k^r,\mathbf{x}-\mathbf{x}')$$

$$\mathbf{\Gamma}^{\rm ME}(\epsilon^r,\mu^r,\omega,\mathbf{x},\mathbf{x}') = -ik^r \mathbf{C}(k^r,\mathbf{x}-\mathbf{x}')$$

$$\mathbf{\Gamma}^{\rm EM}(\epsilon^r,\mu^r,\omega,\mathbf{x},\mathbf{x}') = ik^r\, \mathbf{C}(k^r,\mathbf{x}-\mathbf{x}')$$

$$\mathbf{\Gamma}^{\rm MM}(\epsilon^r,\mu^r,\omega,\mathbf{x},\mathbf{x}') = \frac{ik^r}{Z_0Z^r}\mathbf{G}(k^r,\mathbf{x}-\mathbf{x}')$$

$$\left(Z_0 = \sqrt{\frac{\mu_0}{\epsilon_0}}, \qquad Z^r = \sqrt{\frac{\mu^r}{\epsilon^r}}, \qquad k^r = \sqrt{\mu_0\mu^r\epsilon_0\epsilon^r}\cdot\omega \right)$$

where $\mathbf{G}$, the "photon Green's function," is the solution to the equation

$$\Big[\nabla\times\nabla\times - k^2\Big]\mathbf{G}(k;\mathbf{r}) = \delta(\mathbf{r})\mathbf{1}; \tag{1}$$

and $\mathbf{C}$ is defined by

$$\mathbf{C}(k,\mathbf{r}) = -\frac{1}{ik}\nabla\times\mathbf{G}(k,\mathbf{r}). \tag{2}$$

(Note that the $\mathbf{\Gamma}$ dyadics depend separately on ϵ,μ, and ω, while $\mathbf{G}$ and $\mathbf{C}$ depend only on the combination $k=\sqrt{\epsilon\mu}\cdot\omega$.)

Explicit expressions for the components of $\mathbf{G}$ and $\mathbf{C}$ are

$$G_{ij}(k,\mathbf{r}) = \frac{e^{ikr}}{4\pi(ik)^2r^3}\left[\Big(1-ikr+(ikr)^2\Big)\delta_{ij} + \Big(-3+3ikr-(ikr)^2\Big)\frac{r_ir_j}{r^2}\right]$$

$$C_{ij}(k,\mathbf{r}) = \frac{e^{ikr}}{4\pi(ik)r^3}\varepsilon_{ijk}r_k\Big(-1+ikr\Big)$$

These may also be written in the form

$$G_{ij}(k,\mathbf{r}) = \Big[\delta_{ij}+\frac{1}{k^2}\partial_i\partial_j\Big]G_0(k,\mathbf{r}), \qquad C_{ij}(k,\mathbf{r}) = +\frac{1}{ik}\varepsilon_{ijl}\partial_l G_0(k,\mathbf{r}) \tag{3}$$

where G_0 is the scalar Green's function for the Helmholtz equation,

$$G_0(k;\mathbf{r}) = \frac{e^{ik|\mathbf{r}|}}{4\pi|\mathbf{r}|} \tag{4}$$

which satisfies

$$\Big[\nabla^2 + k^2\Big] G_0(k;\mathbf{r}) = \delta(\mathbf{r}).$$

With these expressions, we can verify that equation (2) is actually just the first half of a pair of reciprocal curl identities relating $\mathbf{G}$ and $\mathbf{C}$:

$$\frac{1}{ik}\nabla\times\mathbf{G} = -\mathbf{C}, \qquad \frac{1}{ik}\nabla\times\mathbf{C} = \mathbf{G}. \tag{5}$$

(As usual with tensors and dyadics, the vector notation here is suggestive but vague; the precise meaning of (2) is

$$\frac{1}{ik}\varepsilon_{iAB}\partial_A G_{Bj} = -C_{ij}, \qquad \frac{1}{ik}\varepsilon_{iAB}\partial_A C_{Bj} = G_{ij}.) \tag{6}$$

Shorthand In what follows, an equation like

$$E_i(\mathbf{x},\omega) = \int_{\mathcal{S}} \Gamma_{ij}^{\text{EE}}(\epsilon^r,\mu^r;\omega;\mathbf{x},\mathbf{x}')K_j(\mathbf{x}')\,d\mathbf{x}'$$

will often be abbreviated to read

$$\mathbf{E}(\mathbf{x}) = \int_{\mathcal{S}} \mathbf{\Gamma}^{\text{EE}}(\mathcal{R}^r;\mathbf{x},\mathbf{x}')\cdot\mathbf{K}(\mathbf{x}')\,d\mathbf{x}'$$

(with ω arguments suppressed and the dependence on ϵ^r,μ^r condensed into a dependence on the region $\mathcal{R}^r$), or even abbreviated further to read

$$\mathbf{E} = \mathbf{\Gamma}^{\text{EE}}(\mathcal{R}^r)\star\mathbf{K}$$

where $\star$ denotes a convolution operation.

4 Computation of the fields in LIBSCUFF geometries

Using the fields of individual basis functions as discussed in the previous section, we can compute the total **E** and **H** fields at arbitrary points in a SCUFF-EM geometry.

4.1 The simplest case

The simplest case to consider is that in which we have a single compact body $\mathcal{B}$ in vacuum; let the body surface be $\mathcal{S} = \partial\mathcal{B}$ and suppose the incident fields arise from sources lying outside $\mathcal{B}$. Let the surface-current coefficients be $\{\mathbf{k}_\alpha, \mathbf{n}_\alpha\}$, so that the electric and magnetic surface currents are

$$\mathbf{K}(\mathbf{x}) = \sum_\alpha k_\alpha \mathbf{b}_\alpha(\mathbf{x}), \qquad \mathbf{N}(\mathbf{x}) = \sum_\alpha n_\alpha \mathbf{b}_\alpha(\mathbf{x})$$

where $\{\mathbf{b}_\alpha\}$ is the set of RWG basis functions on surface $\partial\mathcal{B}$. Then the fields at a point outside $\mathcal{B}$ are

$$\mathbf{E}(\mathbf{x}) = \mathbf{E}^{\rm inc}(\mathbf{x}) + \sum_\alpha \Big\{ ik_0 Z_0 k_\alpha \mathbf{e}_\alpha(k_0;\mathbf{x}) - n_\alpha \mathbf{h}_\alpha(k_0;\mathbf{x}) \Big\} \tag{7a}$$

$$\mathbf{H}(\mathbf{x}) = \mathbf{H}^{\rm inc}(\mathbf{x}) + \sum_\alpha \Big\{ k_\alpha \mathbf{h}_\alpha(k_0;\mathbf{x}) + \frac{ik_0}{Z_0} n_\alpha \mathbf{e}_\alpha(k_0;\mathbf{x}) \Big\}. \tag{7b}$$

The fields at a point inside $\mathcal{B}$ are

$$\mathbf{E}(\mathbf{x}) = -\sum_\alpha \Big\{ ik_1 Z_1 k_\alpha \mathbf{e}_\alpha(k_1;\mathbf{x}) - n_\alpha \mathbf{h}_\alpha(k_1;\mathbf{x}) \Big\} \tag{8a}$$

$$\mathbf{H}(\mathbf{x}) = -\sum_\alpha \Big\{ k_\alpha \mathbf{h}_\alpha(k_1;\mathbf{x}) + \frac{ik_1}{Z_1} n_\alpha \mathbf{e}_\alpha(k_1;\mathbf{x}) \Big\}. \tag{8b}$$

Note the following differences between (7) and (8):

- The incident fields contribute to (7) but not to (8).
- Equation (8) involves a minus sign that is not present in (7).
- Equation (7) involves the vacuum wavenumber $k_0 = \omega/c$ and the vacuum wave impedance $Z_0 \approx 377\,\Omega$. Equation (8) involves the wavenumber $k_1 = \sqrt{\epsilon^r \mu^r} k_0$ and wave impedance $Z_1 = \sqrt{\frac{\mu^r}{\epsilon^r}} Z_0$ for the body interior. (Here $\{\epsilon^r, \mu^r\}$ are the relative permittivity and permeability of the medium inside body $\mathcal{B}$ at the frequency in question.)

4.2 The general case

The previous discussion was for the simplest case of a single compact body in vacuum with incident-field sources lying outside the body. The generalization to more complicated cases is straighforward.

Figure 5: Contributions of objects to the scattered fields at an arbitrary point $\mathbf{x}$. Objects $\mathcal{O}_\beta$ and $\mathcal{O}_\gamma$ contribute to the field at $\mathbf{x}$ "with a plus sign" (cf. equation 9). Object $\mathcal{O}_\alpha$ contributes to the field at $\mathbf{x}$ "with a minus sign." Objects $\mathcal{O}_\delta$ and $\mathcal{O}_\lambda$ do not contribute to the field at $\mathbf{x}$.

Consider a point $\mathbf{x}$ in some region $\mathcal{R}$ of a LIBSCUFF geometry. In general, $\mathcal{R}$ will be bounded by some collection of surfaces $\{\mathcal{S}^s\}$. Let's subdivide the set of surfaces bounding $\mathcal{R}$ into two groups: a first set $\{\mathcal{S}^\alpha\}$ for which $\mathcal{R}$ is the *exterior* surface, and a second set $\{\mathcal{S}^\beta\}$ for which $\mathcal{R}$ is the *interior* surface. Then the electric field at $\mathbf{x}$ is

$$\begin{aligned} E_i(\mathbf{x}) = & \sum_\alpha \int_{\mathcal{S}^\alpha} \Big\{ \Gamma_{ij}^{\text{EE}}(\mathcal{R};\mathbf{x},\mathbf{x}') K_j(\mathbf{x}') + \Gamma_{ij}^{\text{EM}}(\mathcal{R};\mathbf{x},\mathbf{x}') N_j(\mathbf{x}') \Big\} \, d\mathbf{x}' \\ & - \sum_\beta \int_{\mathcal{S}^\beta} \Big\{ \Gamma_{ij}^{\text{EE}}(\mathcal{R};\mathbf{x},\mathbf{x}') K_j(\mathbf{x}') + \Gamma_{ij}^{\text{EM}}(\mathcal{R};\mathbf{x},\mathbf{x}') N_j(\mathbf{x}') \Big\} \, d\mathbf{x}' \\ & + E_i^{\text{inc},r}(\mathbf{x}). \end{aligned} \tag{9}$$

In this equation, $\mathbf{E}^{\text{inc},r}$ is the field due to any incident field sources that lie inside the region $\mathcal{R}^r$. (The $\mathbf{H}$ fields are given by identical relations with $\{\Gamma^{\text{EE}}, \Gamma^{\text{EM}}, E^{\text{inc},r}\} \to \{\Gamma^{\text{ME}}, \Gamma^{\text{MM}}, H^{\text{inc},r}\}$.)

Note the following points with respect to equation (9):

- Sources on surfaces $\mathcal{S}_\alpha$ for which $\mathcal{R}$ is the exterior medium contribute to the fields at $\mathbf{x}$ with a positive sign. Sources on surfaces $\mathcal{S}_\beta$ for which $\mathcal{R}$ is the interior medium contribute to the fields at $\mathbf{x}$ with a negative sign.

- In each line of (9), (i.e. regardless of the surface over which we are integrating) the Green's functions used to compute the fields at $\mathbf{x}$ are the Green's functions for the homogeneous region $\mathcal{R}$ containing $\mathbf{x}$. The material properties of other regions are not referenced.

5 BEM Formulations in LIBSCUFF

In previous sections we discussed how LIBSCUFF represents surface currents and how LIBSCUFF uses surface currents to compute scattered fields. In this section we discuss how LIBSCUFF actually computes the surface currents for a given incident field. To this end, LIBSCUFF employs a variety of BEM formulations, some of which may coexist in a single problem.

5.1 Continuous forms of the integral equations solved by LIBSCUFF

5.1.1 The equation imposed at points on PEC surfaces

For PEC surfaces, LIBSCUFF imposes the *electric field integral equation* (EFIE). This means that at each point $\mathbf{x}$ on a PEC surface $\mathcal{S}$ we require that the tangential components of the total (incident + scattered) field vanish:

$$\hat{\mathbf{n}} \times \mathbf{E}^{\rm total}(\mathbf{x}) = 0, \qquad \mathbf{x} \in \mathcal{S} \tag{10}$$

where $\hat{\mathbf{n}}$ is the normal to the object surface at $\mathbf{x}$.

To obtain an integral equation from (10), suppose that $\mathcal{S}$ is embedded in a homogeneous material region $\mathcal{R}$. Then the total field in (10) is a sum of scattered and incident contributions; the former involve convolutions of the surface-current distributions on all surfaces bounding $\mathcal{R}$ (including $\mathcal{S}$ plus any other surfaces that may be part of the boundary of $\mathcal{R}$), while the latter involve only those incident-field sources lying interior to $\mathcal{R}$. Equation (10) then reads

$$\sum_{\mathcal{S}_s \subset \partial\mathcal{R}} {\rm sgn}(\mathcal{S}_s, R) \oint_{\mathcal{S}_s} \begin{pmatrix} \mathbf{\Gamma}^{\rm EE}(\mathcal{R}) & \mathbf{\Gamma}^{\rm EM}(\mathcal{R}) \\ \mathbf{\Gamma}^{\rm ME}(\mathcal{R}) & \mathbf{\Gamma}^{\rm MM}(\mathcal{R}) \end{pmatrix} \begin{pmatrix} \mathbf{K} \\ \mathbf{N} \end{pmatrix} dA = -\begin{pmatrix} \mathbf{E}^{{\rm inc},r} \\ \mathbf{H}^{{\rm inc},r} \end{pmatrix} \tag{11}$$

or, in convenient shorthand,

$$\sum_{\mathcal{S}_s \subset \partial\mathcal{R}} {\rm sgn}(\mathcal{S}_s, R) \left[\begin{pmatrix} \mathbf{\Gamma}^{\rm EE}(\mathcal{R}) & \mathbf{\Gamma}^{\rm EM}(\mathcal{R}) \\ \mathbf{\Gamma}^{\rm ME}(\mathcal{R}) & \mathbf{\Gamma}^{\rm MM}(\mathcal{R}) \end{pmatrix} \star \begin{pmatrix} \mathbf{K}_s \\ \mathbf{N}_s \end{pmatrix} \right] = -\begin{pmatrix} \mathbf{E}^{{\rm inc},r} \\ \mathbf{H}^{{\rm inc},r} \end{pmatrix} \tag{12}$$

where the sum is over all surfaces $\mathcal{S}_s$ that constitute the boundary $\partial\mathcal{R}$ of the region $\mathcal{R}$ (including $\mathcal{S}$), $\star$ denotes convolution, the s subscript on $\mathbf{K}, \mathbf{N}$ indicates the restriction of the current distributions to $\mathcal{S}_s$, and

$$ {\rm sgn}(\mathcal{S}, \mathcal{R}) \equiv \begin{cases} +1 & \text{if } \mathcal{R} \text{ is the "exterior" region for } \mathcal{S} \\ -1 & \text{if } \mathcal{R} \text{ is the "interior" region for } \mathcal{S}. \end{cases}$$

As discussed in Section 1, the notions of "exterior" and "interior" are defined even when $\mathcal{S}$ is an open surface; in that case its "exterior" region is the region into which its surface normal points.

Note that any PEC surfaces in the sum in (71), including $\mathcal{S}$ itself, have $\mathbf{N} = 0$ identically.

Note that equation (71) may be written using a shorthand notation:

$$\sum_{\mathcal{S}_s \subset \partial\mathcal{R}} \mathrm{sgn}\big(\mathcal{S}_s, \mathcal{R}\big) \Big[\boldsymbol{\mathcal{G}}(\mathcal{R}) \star \boldsymbol{\mathcal{C}}_s \Big] = -\boldsymbol{\mathcal{F}}^{\mathrm{inc},r} \tag{13}$$

where $\boldsymbol{\mathcal{C}}$, $\boldsymbol{\mathcal{F}}$, and $\boldsymbol{\mathcal{G}}$ denote six-vector surface currents, six-vector fields, and 6×6 dyadic Green's functions:

$$\boldsymbol{\mathcal{C}} \equiv \begin{pmatrix} \mathbf{K} \\ \mathbf{N} \end{pmatrix}, \qquad \boldsymbol{\mathcal{F}} \equiv \begin{pmatrix} \mathbf{E} \\ \mathbf{H} \end{pmatrix}, \qquad \boldsymbol{\mathcal{G}}(\mathcal{R}) \equiv \begin{pmatrix} \boldsymbol{\Gamma}^{\mathrm{EE}}(\mathcal{R}) & \boldsymbol{\Gamma}^{\mathrm{EM}}(\mathcal{R}) \\ \boldsymbol{\Gamma}^{\mathrm{ME}}(\mathcal{R}) & \boldsymbol{\Gamma}^{\mathrm{MM}}(\mathcal{R}) \end{pmatrix}.$$

We will use this 6-vector shorthand notation frequently in what follows.

5.1.2 The equation imposed at points on dielectric object surfaces: PMCHWT formulation

By default, LIBSCUFF adopts the PMCHWT formulation of the BEM for dielectric surfaces $\mathcal{S}$. (Alternative formulations may be selected by setting internal LIBSCUFF variables; see below.) In the PMCHWT formulation, we require that, at each point $\mathbf{x} \in \mathcal{S}$, the tangential components of the total $\mathbf{E}$ and $\mathbf{H}$ fields be continuous as we pass through $\mathcal{S}$:

$$\lim_{\eta\to 0} \Big[\mathbf{E}^{\mathrm{total}}(\mathbf{x} + \eta\hat{\mathbf{n}}) - \mathbf{E}^{\mathrm{total}}(\mathbf{x} - \eta\hat{\mathbf{n}}) \Big]_{\parallel} = 0 \tag{14a}$$

$$\lim_{\eta\to 0} \Big[\mathbf{H}^{\mathrm{total}}(\mathbf{x} + \eta\hat{\mathbf{n}}) - \mathbf{H}^{\mathrm{total}}(\mathbf{x} - \eta\hat{\mathbf{n}}) \Big]_{\parallel} = 0. \tag{14b}$$

where the subscript $\parallel$ extracts the vector components tangential to $\mathcal{S}$ at $\mathbf{x}$.

To write an integral-equation version of this, analogous to (13), let $\mathcal{R}_1$ and $\mathcal{R}_2$ be the two regions at whose interface $\mathcal{S}$ lies, with the surface normal to $\mathcal{S}$ taken to point away from $\mathcal{R}_2$ and into $\mathcal{R}_1$. (Thus, if $\mathcal{S}$ is closed, $\mathcal{R}_1$ is its exterior region and $\mathcal{R}_2$ is its interior region; if $\mathcal{S}$ is not closed then everything else goes through in the same way, just without the classification of $\mathcal{R}_{1,2}$ as interior or exterior). Then the integral-equation version of (14b) reads

$$\begin{aligned} &\sum_{\mathcal{S}_s \subset \partial\mathcal{R}_1} \mathrm{sgn}\big(\mathcal{S}_s, \mathcal{R}_1\big) \Big[\boldsymbol{\mathcal{G}}(\mathcal{R}_1) \star \boldsymbol{\mathcal{C}}_s \Big]_{\parallel} - \sum_{\mathcal{S}_s \subset \partial\mathcal{R}_2} \mathrm{sgn}\big(\mathcal{S}_s, \mathcal{R}_2\big) \Big[\boldsymbol{\mathcal{G}}(\mathcal{R}_2) \star \boldsymbol{\mathcal{C}}_s \Big]_{\parallel} \\ &\qquad = \Big[-\boldsymbol{\mathcal{F}}^{\mathrm{inc},r_1} + \boldsymbol{\mathcal{F}}^{\mathrm{inc},r_2} \Big]_{\parallel} \end{aligned} \tag{15}$$

The RHS of (15) describes the fields contributed by sources inside $\mathcal{R}_2$ minus the fields contributed by sources inside $\mathcal{R}_1$.

Note that, when we consider the contribution made by surface $\mathcal{S}$ itself to the sums on the LHS, we have $\mathrm{sgn}\big(\mathcal{S}, \mathcal{R}_1\big) = -\mathrm{sgn}\big(\mathcal{S}, \mathcal{R}_2\big)$, so the two terms on the LHS wind up *adding*, not subtracting, for that surface.

5.1.3 The equation imposed at points on dielectric object surfaces: N-Müller formulation

The N-Müller formulation is an alternative to the PMCHWT approach that yields a different set of integral equations whose discretization exhibits different numerical behavior.[4] To derive the equations of this formulation, consider a surface $\mathcal{S}$ at the interface of two regions $\mathcal{R}_{1,2}$, and let $\hat{\mathbf{n}}$ be the normal to $\mathcal{S}$ pointing into $\mathcal{R}_1$ and away from $\mathcal{R}_2$.[5] One way to express the surface currents is to compute the total fields in $\mathcal{R}_1$ at points approaching the surface from within $\mathcal{R}_1$:

$$\begin{pmatrix} \mathbf{K}(\mathbf{x}) \\ \mathbf{N}(\mathbf{x}) \end{pmatrix} = \lim_{\eta\to 0} \begin{pmatrix} +\hat{\mathbf{n}}\times\mathbf{H}^{\rm tot}\big(\mathbf{x}+\eta\hat{\mathbf{n}}\big) \\ -\hat{\mathbf{n}}\times\mathbf{E}^{\rm tot}\big(\mathbf{x}+\eta\hat{\mathbf{n}}\big) \end{pmatrix}$$

or, using the 6-vector notation introduced above,

$$\begin{aligned} \boldsymbol{\mathcal{C}} &= \lim_{\eta\to 0} \boldsymbol{\mathcal{N}}\boldsymbol{\mathcal{F}}\big(\mathbf{x}+\eta\hat{\mathbf{n}}\big) \\ &= \lim_{\eta\to 0} \boldsymbol{\mathcal{N}}\Big[\boldsymbol{\mathcal{F}}^{{\rm inc},r_1}\big(\mathbf{x}+\eta\hat{\mathbf{n}}\big) \;+\; \boldsymbol{\mathcal{G}}(\mathcal{R}_1)\star\boldsymbol{\mathcal{C}}\Big] \end{aligned} \tag{16}$$

where

$$\boldsymbol{\mathcal{N}} = \begin{pmatrix} 0 & \hat{\mathbf{n}}\times \\ -\hat{\mathbf{n}}\times & 0 \end{pmatrix}$$

and again $\boldsymbol{\mathcal{F}}^{{\rm inc},r_1}$ are the incident fields arising only from those field sources inside $\mathcal{R}_1$.

On the other hand, another way to derive the same surface currents is to compute the total fields in $\mathcal{R}_2$ at points approaching the surface from within $\mathcal{R}_2$:

$$\boldsymbol{\mathcal{C}} = \boldsymbol{\mathcal{N}}\Big[\boldsymbol{\mathcal{F}}^{{\rm inc},r_2}\big(\mathbf{x}-\eta\hat{\mathbf{n}}\big) \;-\; \boldsymbol{\mathcal{G}}(\mathcal{R}_2)\star\boldsymbol{\mathcal{C}}\Big] \tag{17}$$

Equation (16) and (17) are two distinct equations that must hold simultaneously. If we subtract equation (17) from (16) and operate on both sides with $-\boldsymbol{\mathcal{N}}$, we recover the PMCHWT equation (15). On the other hand, if we multiply (16) by $\boldsymbol{\chi}_1$ and (16) by $\boldsymbol{\chi}_2$—where $\boldsymbol{\chi}_r$ is the 6×6 constant diagonal matrix

$$\boldsymbol{\chi}_r = \begin{pmatrix} \mu_r & 0 \\ 0 & -\epsilon_r \end{pmatrix}$$

with ϵ_r, μ_r the relative material properties of region $\mathcal{R}$—and *add* the two equations instead of subtracting, we obtain

$$\Big(\boldsymbol{\chi}_1+\boldsymbol{\chi}_2\Big)\boldsymbol{\mathcal{C}} = \boldsymbol{\chi}_1\boldsymbol{\mathcal{N}}\boldsymbol{\mathcal{F}}^{{\rm inc},r_1} + \boldsymbol{\chi}_2\boldsymbol{\mathcal{N}}\boldsymbol{\mathcal{F}}^{{\rm inc},r_2} + \Big[\boldsymbol{\chi}_1\boldsymbol{\mathcal{N}}\boldsymbol{\mathcal{G}}_1 - \boldsymbol{\chi}_2\boldsymbol{\mathcal{N}}\boldsymbol{\mathcal{G}}_2\Big]\star\boldsymbol{\mathcal{C}}$$

[4] P. Yla-Oijala and M. Taskinen, "Well-conditioned Müller formulation for electromagnetic scattering by dielectric objects," *IEEE Transactions on Antennas and Propagation*, **53** 3316 (2005)

[5] In contrast to other derivations, such as that of the previous footnote, I do *not* use two different symbols to denote the two opposite orientations of the surface normal vector. Throughout this derivation my $\hat{\mathbf{n}}$ vector points always in the *same* direction, namely, out of $\mathcal{R}_2$ into $\mathcal{R}_1$. Similarly, there are not two different $\boldsymbol{\mathcal{N}}$ matrices; there is only one $\boldsymbol{\mathcal{N}}$ matrix.

or, breaking out the 3x3 block components,

$$\begin{pmatrix}(\mu_1+\mu_2)\mathbf{K}\\ -(\epsilon_1+\epsilon_2)\mathbf{N}\end{pmatrix} - \begin{pmatrix} \hat{\mathbf{n}}\times\left[\mu_1\mathbf{\Gamma}_1^{\rm ME}-\mu_2\mathbf{\Gamma}_2^{\rm ME}\right] & \hat{\mathbf{n}}\times\left[\mu_1\mathbf{\Gamma}_1^{\rm MM}-\mu_2\mathbf{\Gamma}_2^{\rm MM}\right] \\ \hat{\mathbf{n}}\times\left[\epsilon_1\mathbf{\Gamma}_1^{\rm EE}-\epsilon_2\mathbf{\Gamma}_2^{\rm EE}\right] & \hat{\mathbf{n}}\times\left[\epsilon_1\mathbf{\Gamma}_1^{\rm EM}-\epsilon_2\mathbf{\Gamma}_2^{\rm EM}\right] \end{pmatrix}\star\begin{pmatrix}\mathbf{K}\\ \mathbf{N}\end{pmatrix}$$
$$= \begin{pmatrix} \hat{\mathbf{n}}\times\left[\mu_1\mathbf{H}^{{\rm inc},r_1}+\mu_2\mathbf{H}^{{\rm inc},r_2}\right] \\ \hat{\mathbf{n}}\times\left[\epsilon_1\mathbf{E}^{{\rm inc},r_1}+\epsilon_2\mathbf{E}^{{\rm inc},r_2}\right] \end{pmatrix}. \tag{18}$$

There is a subtlety in equation (18) that is not present in (15): In evaluating the convolutions on the LHS of (18), we must account for the $\delta-$function singularities in $\mathbf{\Gamma}^{\rm ME}$ and $\mathbf{\Gamma}^{\rm EM}$. [These terms *cancel* out of (15), which is why we didn't need to consider them above]. I think the easiest way to work out what these are is to consider the magnetic field due to an infinite constant sheet of $\mathbf{x}$-directed electric surface current $\mathbf{K}$ confined to the xy plane. Then, by a simple application of the right-hand rule, the magnetic field in the *upper* half space points in the *negative* y-direction, while the magnetic field in the *lower* half space points in the *positive* y-direction. Let the upper (lower) half-space be $\mathcal{R}_1$ ($\mathcal{R}_2$). Then we have

$$\hat{\mathbf{n}}=\hat{\mathbf{z}}, \qquad \mathbf{K}=K\hat{\mathbf{x}}.$$

The magnetic field in the upper half-space is

$$\mathbf{\Gamma}_1^{\rm ME}\star\mathbf{K} = -\frac{1}{2}K\hat{\mathbf{y}}, \qquad z\geq 0.$$

In the lower half-space, we find instead

$$\mathbf{\Gamma}_2^{\rm ME}\star\mathbf{K} = +\frac{1}{2}K\hat{\mathbf{y}}, \qquad z\leq 0.$$

Thus, at $z=0$, we find

$$\begin{aligned}\hat{\mathbf{n}}\times\left[\mu_1\mathbf{\Gamma}_1^{\rm ME}-\mu_2\mathbf{\Gamma}_2^{\rm ME}\right]\star\mathbf{K} &= -\frac{(\mu_1+\mu_2)K}{2}\hat{\mathbf{z}}\times\hat{\mathbf{y}} \\ &= +\frac{(\mu_1+\mu_2)K}{2}\hat{\mathbf{x}} \\ &= \frac{(\mu_1+\mu_2)}{2}\mathbf{K}. \end{aligned}\tag{19a}$$

and by analogous arguments we find

$$\hat{\mathbf{n}}\times\left[\epsilon_1\mathbf{\Gamma}_1^{\rm EM}-\epsilon_2\mathbf{\Gamma}_2^{\rm EM}\right]\star\mathbf{N} = -\frac{(\epsilon_1+\epsilon_2)}{2}\mathbf{N}. \tag{19b}$$

Using equations (19), we can rewrite the N-Müller system (18) in a way that

involves only the non-singular parts of the dyadic Green's functions:

$$\frac{1}{2}\begin{pmatrix}(\mu_1+\mu_2)\mathbf{K}\\ -(\epsilon_1+\epsilon_2)\mathbf{N}\end{pmatrix} - \begin{pmatrix} \hat{\mathbf{n}}\times\left[\mu_1\overline{\mathbf{\Gamma}}_1^{\rm ME}-\mu_2\overline{\mathbf{\Gamma}}_2^{\rm ME}\right] & \hat{\mathbf{n}}\times\left[\mu_1\mathbf{\Gamma}_1^{\rm MM}-\mu_2\mathbf{\Gamma}_2^{\rm MM}\right] \\ \hat{\mathbf{n}}\times\left[\epsilon_1\mathbf{\Gamma}_1^{\rm EE}-\epsilon_2\mathbf{\Gamma}_2^{\rm EE}\right] & \hat{\mathbf{n}}\times\left[\epsilon_1\overline{\mathbf{\Gamma}}_1^{\rm EM}-\epsilon_2\overline{\mathbf{\Gamma}}_2^{\rm EM}\right] \end{pmatrix}\star\begin{pmatrix}\mathbf{K}\\ \mathbf{N}\end{pmatrix}$$
$$= \begin{pmatrix} \hat{\mathbf{n}}\times\left[\mu_1\mathbf{H}^{{\rm inc},r_1}+\mu_2\mathbf{H}^{{\rm inc},r_2}\right] \\ \hat{\mathbf{n}}\times\left[\epsilon_1\mathbf{E}^{{\rm inc},r_1}+\epsilon_2\mathbf{E}^{{\rm inc},r_2}\right] \end{pmatrix}. \qquad (20)$$

where $\overline{\mathbf{\Gamma}}^{\rm ME}, \overline{\mathbf{\Gamma}}^{\rm EM}$ denote the relevant DGFs with the singular term neglected; in particular, the diagonal of the second term on the LHS vanishes.

Discretization

$$\mathbf{Mc} = \mathbf{v}$$

$$\mathbf{M} = \mathbf{M}^{(1)} - \mathbf{M}^{(2)}$$
$$M^{(1)}_{\alpha\beta} = \frac{1}{2}\begin{pmatrix} (\mu_1+\mu_2)\langle\mathbf{b}_\alpha,\mathbf{b}_\beta\rangle & 0 \\ 0 & (\epsilon_1+\epsilon_2)\langle\mathbf{b}_\alpha,\mathbf{b}_\beta\rangle \end{pmatrix}$$
$$M^{(2)}_{\alpha\beta} = \begin{pmatrix} -ik_1\mu_1\langle\mathbf{b}_\alpha,\hat{\mathbf{n}}\times\mathbf{C}_1\mathbf{b}_\beta\rangle + ik_2\mu_2\langle\mathbf{b}_\alpha,\hat{\mathbf{n}}\times\mathbf{C}_2\mathbf{b}_\beta\rangle & i\frac{\mu_1 k_1}{Z_0 Z_1}\langle\mathbf{b}_\alpha,\hat{\mathbf{n}}\times\mathbf{G}_1\mathbf{b}_\beta\rangle - i\frac{\mu_2 k_2}{Z_0 Z_2}\langle\mathbf{b}_\alpha,\hat{\mathbf{n}}\times\mathbf{G}_2 \\ ik_1 Z_0 Z_1\epsilon_1\langle\mathbf{b}_\alpha,\hat{\mathbf{n}}\times\mathbf{G}_1\mathbf{b}_\beta\rangle - ik_2 Z_0 Z_2\epsilon_2\langle\mathbf{b}_\alpha,\hat{\mathbf{n}}\times\mathbf{G}_1\mathbf{b}_\beta\rangle & +ik_1\mu_1\langle\mathbf{b}_\alpha,\hat{\mathbf{n}}\times\mathbf{C}_1\mathbf{b}_\beta\rangle - ik_2\mu_2\langle\mathbf{b}_\alpha,\hat{\mathbf{n}}\times\mathbf{C}_2 \end{pmatrix}$$

5.1.4 Modifications for nonzero surface impedance

PEC bodies

In the presence of a nonzero surface impedance $Z_s(\mathbf{x}) > 0$ (corresponding to a finite surface conductivity $G_s(\mathbf{x}) = \frac{1}{Z_s(\mathbf{x})} < \infty$), equation (10) is modified to read

$$\hat{\mathbf{n}}\times\mathbf{E}^{\rm total}(\mathbf{x}) = \frac{1}{G_s(\mathbf{x})}\hat{\mathbf{n}}\times\mathbf{K}(\mathbf{x}) \qquad (21)$$

where $\mathbf{K}(\mathbf{x})$ is the (unknown) electric surface current at $\mathbf{x}$.

Note that we use the symbol G, not σ, for surface conductivity, because this quantity has the dimensions of a conductance (current/voltage), not the dimensions of a conductivity [current/(voltage·length)].

Dielectric bodies, PMCHWT Formulation

In the presence of a nonvanishing surface impedance $Z_s(\mathbf{x})$ (corresponding to a finite surface conductivity, $G_s(\mathbf{x}) = \frac{1}{Z_s(\mathbf{x})} < \infty$), the **E**-field continuity equation

[the first of equations (15)] is unchanged, while the **H**-field continuity equation is modified to read

$$\lim_{\eta\to 0} \hat{\mathbf{n}} \times \Big[\mathbf{H}^{\rm total}(\mathbf{x}+\eta\hat{\mathbf{n}}) - \mathbf{H}^{\rm total}(\mathbf{x}-\eta\hat{\mathbf{n}})\Big] = G(\mathbf{x})\mathbf{E}^{\rm total}(\mathbf{x}) \tag{22a}$$

$$= -G(\mathbf{x})\hat{\mathbf{n}}\times\mathbf{N}(\mathbf{x}) \tag{22b}$$

is the (unknown) magnetic surface current at $\mathbf{x}$.

6 Introduction of the $-Z_0$ Prefactor in the Magnetic Current Expansion

In rough schematic form, the equations derived in the previous section take the form

$$\begin{pmatrix} \mathbf{\Gamma}^{\rm EE} & \mathbf{\Gamma}^{\rm EM} \\ \mathbf{\Gamma}^{\rm ME} & \mathbf{\Gamma}^{\rm MM} \end{pmatrix} * \begin{pmatrix} \mathbf{K} \\ \mathbf{N} \end{pmatrix} = - \begin{pmatrix} \mathbf{E}^{\rm inc} \\ \mathbf{H}^{\rm inc} \end{pmatrix}$$

where $*$ denotes a convolution operation.

The matrix kernel on the LHS is not symmetric because $\mathbf{\Gamma}^{\rm EM} = -\mathbf{\Gamma}^{\rm ME}$. To remedy this, I **(a)** scale the magnetic current by $-1/Z_0$, and then **(b)** divide the upper row of the system by Z_0 to obtain the following symmetric system[6]:

$$\begin{pmatrix} \frac{1}{Z_0}\mathbf{\Gamma}^{\rm EE} & -\mathbf{\Gamma}^{\rm EM} \\ \mathbf{\Gamma}^{\rm ME} & -Z_0\mathbf{\Gamma}^{\rm MM} \end{pmatrix} * \begin{pmatrix} \mathbf{K} \\ -\frac{1}{Z_0}\mathbf{N} \end{pmatrix} = - \begin{pmatrix} \frac{1}{Z_0}\mathbf{E}^{\rm inc} \\ \mathbf{H}^{\rm inc} \end{pmatrix} \tag{23}$$

Equation (23) is the actual linear system solved by LIBSCUFF.

[6] L. N. Medgyesi-Mitschang, J. M. Putnam, and M. B. Gedera, "Generalized method of moments for three-dimensional penetrable scatterers," *J. Opt. Soc. Am. A*, vol. 11, no. 4, pp. 1383–1398, Apr 1994.

7 The Equations Solved by LIBSCUFF: Discrete Forms

Discretization Procedure

LIBSCUFF uses a two-step procedure to discretize the integral equations derived in the previous sections. Briefly, we approximate the $\mathbf{K}$ and $\mathbf{N}$ surface-current distributions as expansions in RWG basis functions, then Galerkin-test the resulting equations again with the RWG basis functions.

In more detail,

1. First, LIBSCUFF approximates surface currents as expansions in RWG basis functions.

   For electric currents on the surfaces of PEC objects, we have the expansion

   $$\mathbf{K}(\mathbf{x}) \approx \sum K_{\alpha n} \mathbf{f}_{\alpha n}(\mathbf{x}) \tag{24a}$$

   where α runs over all PEC objects in the geometry and n runs over all RWG basis functions on object $\mathcal{O}_\alpha$.

   For electric and magnetic currents on the surfaces of dielectric objects, we have the expansions

   $$\mathbf{K}(\mathbf{x}) \approx \sum K_{\beta n} \mathbf{f}_{\beta n}(\mathbf{x}), \qquad \mathbf{N}(\mathbf{x}) \approx -Z_0 \sum N_{\beta n} \mathbf{f}_{\beta n}(\mathbf{x}) \tag{24b}$$

   where β runs over all PEC objects in the geometry and n runs over all RWG basis functions on object $\mathcal{O}_\beta$. (The rationale for the prefactor $-Z_0$ was explained in the previous section).

2. Second, LIBSCUFF obtains one equation for each of the unknown K and N coefficients in (24) by proceeding as follows.

   First, we take the inner product of equation (**??**) with each RWG basis function $\mathbf{f}_{\alpha n}$ defined on the surface of each PEC object. This gives us one equation for each of the $K_{\alpha n}$ coefficients in (24a).

   Second, we take the inner product of equation (**??**) with each RWG basis function $\mathbf{f}_{\beta n}$ defined on the surface of each dielectric object. We associate the resulting equation with the coefficient $K_{\beta n}$ in (24b). Then, we take the inner product of the magnetic analogue of (**??**) (which, as stated above, is identical to (**??**) with the replacements $\{\mathbf{\Gamma}^{\rm EE}, \mathbf{\Gamma}^{\rm EM}\} \to \{\mathbf{\Gamma}^{\rm ME}, \mathbf{\Gamma}^{\rm MM}\}$) with $\mathbf{f}_{\beta n}$) and associate the resulting equation with the coefficient $N_{\beta n}$ in (24b).

Discretized Version of Equation (??)

We consider again the setting of Figure **??**: We have a PEC object $\mathcal{O}_\beta$, embedded in an object $\mathcal{O}_\alpha$ (which may be the environment $\mathcal{O}_e$); also embedded in $\mathcal{O}_\alpha$ are additional PEC object(s) $\mathcal{O}_{\beta'}$ and dielectric object(s) $\mathcal{O}_\gamma$. Inserting expansions (24) into (**??**) and Galerkin-testing with a basis function $\mathbf{f}_{\beta m}$ on

the surface of $\mathcal{O}_\beta$ yields (after dividing both sides of the equation by Z_0 as per equation (23):

$$\begin{aligned}
&\sum_{n=1}^{\texttt{NEdges}(\beta)} \Big\langle \mathbf{f}_{\beta m}\Big|\frac{1}{Z_0}\mathbf{\Gamma}^{\rm EE}(\alpha)\Big|\mathbf{f}_{\beta n}\Big\rangle K_{\beta n} \\
+&\sum_{n=1}^{\texttt{NEdges}(\beta')} \Big\langle \mathbf{f}_{\beta m}\Big|\frac{1}{Z_0}\mathbf{\Gamma}^{\rm EE}(\alpha)\Big|\mathbf{f}_{\beta' n}\Big\rangle K_{\beta' n} \\
+&\sum_{n=1}^{\texttt{NEdges}(\gamma)} \left\{\Big\langle \mathbf{f}_{\beta m}\Big|\frac{1}{Z_0}\mathbf{\Gamma}^{\rm EE}(\alpha)\Big|\mathbf{f}_{\gamma n}\Big\rangle K_{\gamma n} - \Big\langle \mathbf{f}_{\beta m}\Big|\mathbf{\Gamma}^{\rm EM}(\alpha)\Big|\mathbf{f}_{\gamma n}\Big\rangle N_{\gamma n}\right\} \\
-&\sum_{n=1}^{\texttt{NEdges}(\alpha)} \left\{\Big\langle \mathbf{f}_{\beta m}\Big|\frac{1}{Z_0}\mathbf{\Gamma}^{\rm EE}(\alpha)\Big|\mathbf{f}_{\alpha n}\Big\rangle K_{\alpha n} - \Big\langle \mathbf{f}_{\beta m}\Big|\mathbf{\Gamma}^{\rm EM}(\alpha)\Big|\mathbf{f}_{\alpha n}\Big\rangle N_{\alpha n}\right\} \\
&= -\frac{1}{Z_0}\chi_\alpha^{\rm inc}\Big\langle \mathbf{f}_{\beta m}\Big|\mathbf{E}^{\rm inc}\Big\rangle. \qquad (25)
\end{aligned}$$

Discretized Version of Equation (??) and its Magnetic Analogue

Again in the setting of Figure **??**, we Galerkin-test equation (**??**) with a basis function $\mathbf{f}_{\gamma m}$ on the surface of object $\mathcal{O}_\gamma$ to find (again, dividing through by Z_0 as per (23)):

$$\begin{aligned}
&\sum_{n=1}^{\texttt{NEdges}(\gamma)} \left\{\Big\langle \mathbf{f}_{\gamma m}\Big|\frac{1}{Z_0}\mathbf{\Gamma}^{\rm EE}(\alpha)+\frac{1}{Z_0}\mathbf{\Gamma}^{\rm EE}(\gamma)\Big|\mathbf{f}_{\gamma n}\Big\rangle K_{\gamma n} - \Big\langle \mathbf{f}_{\gamma m}\Big|\mathbf{\Gamma}^{\rm EM}(\alpha)+\mathbf{\Gamma}^{\rm EM}(\gamma)\Big|\mathbf{f}_{\gamma n}\Big\rangle N_{\gamma n}\right\} \\
&\sum_{n=1}^{\texttt{NEdges}(\gamma')} \left\{\Big\langle \mathbf{f}_{\gamma m}\Big|\frac{1}{Z_0}\mathbf{\Gamma}^{\rm EE}(\alpha)\Big|\mathbf{f}_{\gamma' n}\Big\rangle K_{\gamma' n} - \Big\langle \mathbf{f}_{\gamma m}\Big|\mathbf{\Gamma}^{\rm EM}(\alpha)\Big|\mathbf{f}_{\gamma' n}\Big\rangle N_{\gamma' n}\right\} \\
+&\sum_{n=1}^{\texttt{NEdges}(\beta)} \Big\langle \mathbf{f}_{\gamma m}\Big|\frac{1}{Z_0}\mathbf{\Gamma}^{\rm EE}(\alpha)\Big|\mathbf{f}_{\beta n}\Big\rangle K_{\beta n} \\
-&\sum_{n=1}^{\texttt{NEdges}(\alpha)} \left\{\Big\langle \mathbf{f}_{\gamma m}\Big|\frac{1}{Z_0}\mathbf{\Gamma}^{\rm EE}(\alpha)\Big|\mathbf{f}_{\alpha n}\Big\rangle K_{\alpha n} - \Big\langle \mathbf{f}_{\gamma m}\Big|\mathbf{\Gamma}^{\rm EM}(\alpha)\Big|\mathbf{f}_{\alpha n}\Big\rangle N_{\alpha n}\right\} \\
-&\sum_{n=1}^{\texttt{NEdges}(\delta)} \left\{\Big\langle \mathbf{f}_{\gamma m}\Big|\frac{1}{Z_0}\mathbf{\Gamma}^{\rm EE}(\gamma)\Big|\mathbf{f}_{\delta n}\Big\rangle K_{\delta n} - \Big\langle \mathbf{f}_{\gamma m}\Big|\mathbf{\Gamma}^{\rm EM}(\gamma)\Big|\mathbf{f}_{\delta n}\Big\rangle N_{\delta n}\right\} \\
&= \frac{1}{Z_0}\Big[\chi_\gamma^{\rm inc}-\chi_\alpha^{\rm inc}\Big]\Big\langle \mathbf{f}_{\gamma m}\Big|\mathbf{E}^{\rm inc}\Big\rangle. \qquad (26a)
\end{aligned}$$

Discretized Version of the Magnetic Analogue of Equation (??)

Finally,, we Galerkin-test the magnetic-field analogue of (**??**) to find

$$\begin{aligned}
&\sum_{n=1}^{\texttt{NEdges}(\gamma)} \left\{ \Big\langle \mathbf{f}_{\gamma m} \Big| \mathbf{\Gamma}^{\rm ME}(\alpha) + \mathbf{\Gamma}^{\rm ME}(\gamma) \Big| \mathbf{f}_{\gamma n} \Big\rangle K_{\gamma n} - \Big\langle \mathbf{f}_{\gamma m} \Big| Z_0\mathbf{\Gamma}^{\rm MM}(\alpha) + Z_0\mathbf{\Gamma}^{\rm MM}(\gamma) \Big| \mathbf{f}_{\gamma n} \Big\rangle N_{\gamma n} \right\} \\
&\sum_{n=1}^{\texttt{NEdges}(\gamma')} \left\{ \Big\langle \mathbf{f}_{\gamma m} \Big| \mathbf{\Gamma}^{\rm ME}(\alpha) \Big| \mathbf{f}_{\gamma' n} \Big\rangle K_{\gamma' n} - \Big\langle \mathbf{f}_{\gamma m} \Big| Z_0\mathbf{\Gamma}^{\rm MM}(\alpha) \Big| \mathbf{f}_{\gamma' n} \Big\rangle N_{\gamma' n} \right\} \\
+ &\sum_{n=1}^{\texttt{NEdges}(\beta)} \Big\langle \mathbf{f}_{\gamma m} \Big| \mathbf{\Gamma}^{\rm ME}(\alpha) \Big| \mathbf{f}_{\beta n} \Big\rangle K_{\beta n} \\
- &\sum_{n=1}^{\texttt{NEdges}(\alpha)} \left\{ \Big\langle \mathbf{f}_{\gamma m} \Big| \mathbf{\Gamma}^{\rm ME}(\alpha) \Big| \mathbf{f}_{\alpha n} \Big\rangle K_{\alpha n} - \Big\langle \mathbf{f}_{\gamma m} \Big| Z_0\mathbf{\Gamma}^{\rm MM}(\alpha) \Big| \mathbf{f}_{\alpha n} \Big\rangle N_{\alpha n} \right\} \\
- &\sum_{n=1}^{\texttt{NEdges}(\delta)} \left\{ \Big\langle \mathbf{f}_{\gamma m} \Big| \mathbf{\Gamma}^{\rm ME}(\gamma) \Big| \mathbf{f}_{\delta n} \Big\rangle K_{\delta n} - \Big\langle \mathbf{f}_{\gamma m} \Big| Z_0\mathbf{\Gamma}^{\rm MM}(\gamma) \Big| \mathbf{f}_{\delta n} \Big\rangle N_{\delta n} \right\} \\
&= \Big[\chi_\gamma^{\rm inc} - \chi_\alpha^{\rm inc} \Big] \Big\langle \mathbf{f}_{\gamma m} \Big| \mathbf{H}^{\rm inc} \Big\rangle. \qquad (26b)
\end{aligned}$$

8 Structure of the BEM System

The discretization procedure of the previous section results in a linear system of the form

$$\Big[\mathbf{M}\Big] \cdot \Big[\mathbf{KN}\Big] = \Big[\mathbf{RHS}\Big] \tag{27}$$

where the vector $\Big[\mathbf{KN}\Big]$ contains the unknown K and N coefficients from equation (24), the matrix $\Big[\mathbf{M}\Big]$ is the "BEM matrix," and the right-hand-side vector $\Big[\mathbf{RHS}\Big]$ depends on the incident fields.

In the remainder of this section we will describe the structure of each of the entities in equation (27).

8.1 Structure of the coefficient vector

The **KN** vector contains the K and N coefficients in (24), ordered as follows:

1. All coefficients for object $\mathcal{O}_1$ come first, followed by all coefficients for object $\mathcal{O}_2$, etc.

   (Object indices correspond with the order in which the objects were specified in the `.rwggeo` file used as input to LIBSCUFF.)

2. Within the portion of the vector corresponding to a dielectric object, the electric and magnetic coefficients for the first RWG basis function come first, followed by the electric and magnetic coefficients for the second RWG basis function, etc.

Thus, for a geometry consisting of object $\mathcal{O}_1$ (PEC) with M interior edges in its surface discretization and object $\mathcal{O}_2$ (dielectric) with N interior edges in its surface discretization, the **KN** vector has dimension $M + 2N$ and looks like

$$\mathbf{KN} = \begin{pmatrix} K_{11} \\ K_{12} \\ \vdots \\ K_{1M} \\ K_{21} \\ N_{21} \\ \vdots \\ K_{2N} \\ N_{2N} \end{pmatrix}.$$

To compute the index of any given coefficient $K_{\alpha n}$ or $N_{\alpha n}$ within the **KN** vector, it is useful first to define functions $\texttt{NBF}(\alpha)$ and $\texttt{BFIndexOffset}(\alpha)$. The former of these is just the number of basis functions on object α, i.e.

$$\texttt{NBF}(\alpha) = \begin{cases} \texttt{NEdges}(\alpha), & \text{if object } \mathcal{O}_\alpha \text{ is PEC} \\ 2 \cdot \texttt{NEdges}(\alpha), & \text{if object } \mathcal{O}_\alpha \text{ is dielectric.} \end{cases}$$

(Here $\texttt{NEdges}(\alpha)$ is the number of interior edges in the surface discretization of object $\mathcal{O}_\alpha$.)

The function $\texttt{BFIndexOffset}(\alpha)$ is the index within the **KN** vector of the first coefficient corresponding to object $\mathcal{O}_\alpha$; thus

$$\begin{aligned}\texttt{BFIndexOffset}(1) &= 1\\ \texttt{BFIndexOffset}(2) &= 1 + \texttt{NBF}(1)\\ \texttt{BFIndexOffset}(3) &= 1 + \texttt{NBF}(1) + \texttt{NBF}(2)\end{aligned}$$

et cetera.

Then I can write the following relations for the indices with the **KN** vector of individual K, N coefficients. (Note that these are one-based indices, which must be translated into zero-based indices for use in `C++` code.)

$$\begin{aligned}\mathcal{I}(K,\alpha,n) &\equiv \text{Index of coefficient } K_{\alpha n} \text{ within the } \mathbf{KN} \text{ vector}\\ &= \begin{cases}\texttt{BFIndexOffset}(\alpha) + n - 1, & \text{if } \mathcal{O}_\alpha \text{ is PEC}\\ \texttt{BFIndexOffset}(\alpha) + 2(n-1), & \text{if } \mathcal{O}_\alpha \text{ is dielectric}\end{cases}\\ \mathcal{I}(N,\alpha,n) &\equiv \text{Index of coefficient } N_{\alpha n} \text{ within the } \mathbf{KN} \text{ vector}\\ &= \texttt{BFIndexOffset}(\alpha) + 2(n-1) + 1.\end{aligned}$$

8.2 Structure of the RHS vector

The structure of the RHS vector mirrors the structure of the coefficient vector:

- If the nth element of the coefficient vector is a K coefficient (i.e. the electric surface-current expansion coefficient associated with some RWG basis function $\mathbf{b}$), then the nth element of the RHS vector is minus the inner product of the incident electric field with $\mathbf{b}$, divided by Z_0.
- If the nth element of the coefficient vector is an N coefficient (i.e. the magnetic surface-current expansion coefficient associated with some RWG basis function $\mathbf{b}$), then the nth element of the RHS vector is minus the inner product of the incident magnetic field with $\mathbf{b}$.

For the example considered above, consisting of a PEC surface with M interior edges and a dielectric surface with N interior edges, the elements of the RHS vector would be

$$\mathbf{RHS} = -\begin{pmatrix} \langle \mathbf{E}^{\rm inc}, \mathbf{b}_{11}\rangle/Z_0 \\ \langle \mathbf{E}^{\rm inc}, \mathbf{b}_{12}\rangle/Z_0 \\ \vdots \\ \langle \mathbf{E}^{\rm inc}, \mathbf{b}_{1M}\rangle/Z_0 \\ \langle \mathbf{E}^{\rm inc}, \mathbf{b}_{21}\rangle/Z_0 \\ \langle \mathbf{H}^{\rm inc}, \mathbf{b}_{21}\rangle \\ \langle \mathbf{E}^{\rm inc}, \mathbf{b}_{22}\rangle/Z_0 \\ \vdots \\ \langle \mathbf{H}^{\rm inc}, \mathbf{b}_{2N}\rangle \end{pmatrix}.$$

8.3 Structure of the BEM matrix

Consider two basis functions: $\mathbf{f}_{\alpha m}$, corresponding to the mth interior edge of object $\mathcal{O}_\alpha$, and $\mathbf{f}_{\beta n}$, corresponding to the nth interior edge of object $\mathcal{O}_\beta$.

Let $\mathbf{A}$ be the index of the medium through which the objects interact. (If we have `NObj` objects in our geometry, then either $1 \le \mathbf{A} \le$ `NObj` or else $\mathbf{A} = e$ for the external medium.) Thus,

- If $\mathcal{O}_\alpha$ is contained in $\mathcal{O}_\beta$, then $\mathbf{A} = \beta$.
- If $\mathcal{O}_\beta$ is contained in $\mathcal{O}_\alpha$, then $\mathbf{A} = \alpha$.
- If $\mathcal{O}_\alpha$ and $\mathcal{O}_\alpha$ are both contained in the same object $\mathcal{O}_\gamma$ (which may be the external medium $\mathcal{O}_e$), then then $\mathbf{A} = \gamma$.
- If none of the above are true, then the two objects do not interact and the corresponding block of the BEM matrix is zero.

Define a symbol `Sign` to have value -1 in the first two cases (i.e. when one of $\mathcal{O}_\alpha$, $\mathcal{O}_\beta$ is contained inside the other), while `Sign` $= +1$ otherwise.

Then the two basis elements contribute a 1×1, 1×2, 2×1, or 2×2 block of matrix elements to the BEM matrix, which may be determined by looking at equations (25) and (26) as follows:

1. **Both objects are PEC:**

$$M\Big(\mathcal{I}^K_{\alpha m}, \mathcal{I}^K_{\beta n}\Big) = \frac{1}{Z_0}\Big\langle \mathbf{f}_{\alpha m}\Big|\mathbf{\Gamma}^{\rm EE}(\mathbf{A})\Big|\mathbf{f}_{\beta n}\Big\rangle = ik^{\rm A}Z^{\rm A}\Big\langle \mathbf{f}_{\alpha m}\Big|\mathbf{G}(k^{\rm A})\Big|\mathbf{f}_{\beta n}\Big\rangle$$

2. $\mathcal{O}_\alpha$ **is PEC,** $\mathcal{O}_\beta$ **is dielectric:**

$$\begin{aligned} M\Big(\mathcal{I}^K_{\alpha m}, \mathcal{I}^K_{\beta n}\Big) &= \frac{\texttt{Sign}}{Z_0}\Big\langle \mathbf{f}_{\alpha m}\Big|\mathbf{\Gamma}^{\rm EE}(\mathbf{A})\Big|\mathbf{f}_{\beta n}\Big\rangle &&= \texttt{Sign}\cdot ik^{\rm A}Z^{\rm A}\Big\langle \mathbf{f}_{\alpha m}\Big|\mathbf{G}(k^{\rm A})\Big|\mathbf{f}_{\beta n}\Big\rangle \\ M\Big(\mathcal{I}^K_{\alpha m}, \mathcal{I}^N_{\beta n}\Big) &= -\texttt{Sign}\cdot\Big\langle \mathbf{f}_{\alpha m}\Big|\mathbf{\Gamma}^{\rm EM}(\mathbf{A})\Big|\mathbf{f}_{\beta n}\Big\rangle &&= -\texttt{Sign}\cdot ik^{\rm A}\Big\langle \mathbf{f}_{\alpha m}\Big|\mathbf{C}(k^{\rm A})\Big|\mathbf{f}_{\beta n}\Big\rangle \end{aligned}$$

3. $\mathcal{O}_\alpha$ **is dielectric,** $\mathcal{O}_\beta$ **is PEC:**

$$\begin{aligned} M\Big(\mathcal{I}^K_{\alpha m},\mathcal{I}^K_{\beta n}\Big) &= \frac{\texttt{Sign}}{Z_0}\Big\langle \mathbf{f}_{\alpha m}\Big|\mathbf{\Gamma}^{\rm EE}(\mathbf{A})\Big|\mathbf{f}_{\beta n}\Big\rangle &= \texttt{Sign}\cdot ik^{\rm A}Z^{\rm A}\Big\langle \mathbf{f}_{\alpha m}\Big|\mathbf{G}(k^{\rm A})\Big|\mathbf{f}_{\beta n}\Big\rangle \\ M\Big(\mathcal{I}^N_{\alpha m},\mathcal{I}^K_{\beta n}\Big) &= \texttt{Sign}\cdot\Big\langle \mathbf{f}_{\alpha m}\Big|\mathbf{\Gamma}^{\rm ME}(\mathbf{A})\Big|\mathbf{f}_{\beta n}\Big\rangle &= -\texttt{Sign}\cdot ik^{\rm A}\Big\langle \mathbf{f}_{\alpha m}\Big|\mathbf{C}(k^{\rm A})\Big|\mathbf{f}_{\beta n}\Big\rangle \end{aligned}$$

4. $\mathcal{O}_\alpha,\mathcal{O}_\beta$ **are both dielectric and** $\mathcal{O}_\alpha\neq\mathcal{O}_\beta$**:**

$$\begin{aligned} M\Big(\mathcal{I}^K_{\alpha m},\mathcal{I}^K_{\beta n}\Big) &= \frac{\texttt{Sign}}{Z_0}\Big\langle \mathbf{f}_{\alpha m}\Big|\mathbf{\Gamma}^{\rm EE}(\mathbf{A})\Big|\mathbf{f}_{\beta n}\Big\rangle &= \texttt{Sign}\cdot ik^{\rm A}Z^{\rm A}\Big\langle \mathbf{f}_{\alpha m}\Big|\mathbf{G}(k^{\rm A})\Big|\mathbf{f}_{\beta n}\Big\rangle \\ M\Big(\mathcal{I}^K_{\alpha m},\mathcal{I}^N_{\beta n}\Big) &= -\texttt{Sign}\cdot\Big\langle \mathbf{f}_{\alpha m}\Big|\mathbf{\Gamma}^{\rm EM}(\mathbf{A})\Big|\mathbf{f}_{\beta n}\Big\rangle &= -\texttt{Sign}\cdot ik^{\rm A}\Big\langle \mathbf{f}_{\alpha m}\Big|\mathbf{C}(k^{\rm A})\Big|\mathbf{f}_{\beta n}\Big\rangle \\ M\Big(\mathcal{I}^N_{\alpha m},\mathcal{I}^K_{\beta n}\Big) &= \texttt{Sign}\cdot\Big\langle \mathbf{f}_{\alpha m}\Big|\mathbf{\Gamma}^{\rm ME}(\mathbf{A})\Big|\mathbf{f}_{\beta n}\Big\rangle &= -\texttt{Sign}\cdot ik^{\rm A}\Big\langle \mathbf{f}_{\alpha m}\Big|\mathbf{C}(k^{\rm A})\Big|\mathbf{f}_{\beta n}\Big\rangle \\ M\Big(\mathcal{I}^N_{\alpha m},\mathcal{I}^N_{\beta n}\Big) &= -\texttt{Sign}\cdot Z_0\Big\langle \mathbf{f}_{\alpha m}\Big|\mathbf{\Gamma}^{\rm MM}(\mathbf{A})\Big|\mathbf{f}_{\beta n}\Big\rangle &= -\frac{\texttt{Sign}\cdot ik^{\rm A}}{Z^{\rm A}}\Big\langle \mathbf{f}_{\alpha m}\Big|\mathbf{G}(k^{\rm A})\Big|\mathbf{f}_{\beta n}\Big\rangle \end{aligned}$$

5. $\mathcal{O}_\alpha,\mathcal{O}_\beta$ **are both dielectric and** $\mathcal{O}_\alpha=\mathcal{O}_\beta$**:**

This case is identical to the previous case, but now the matrix elements are augmented by additional contributions describing the basis functions interacting through the medium inside the object. Let the index of this medium be $\mathbf{B}$. (We have $\mathbf{B}=\alpha=\beta$.) Then the matrix elements are

$$\begin{aligned} M\Big(\mathcal{I}^K_{\alpha m},\mathcal{I}^K_{\beta n}\Big) &= \frac{1}{Z_0}\Big\langle \mathbf{f}_{\alpha m}\Big|\mathbf{\Gamma}^{\rm EE}(\mathbf{A})+\mathbf{\Gamma}^{\rm EE}(\mathbf{B})\Big|\mathbf{f}_{\beta n}\Big\rangle \\ &= ik^{\rm A}Z^{\rm A}\Big\langle \mathbf{f}_{\alpha m}\Big|\mathbf{G}(k^{\rm A})\Big|\mathbf{f}_{\beta n}\Big\rangle + ik^{\rm B}Z^{\rm B}\Big\langle \mathbf{f}_{\alpha m}\Big|\mathbf{G}(k^{\rm B})\Big|\mathbf{f}_{\beta n}\Big\rangle \\ M\Big(\mathcal{I}^K_{\alpha m},\mathcal{I}^N_{\beta n}\Big) &= -\Big\langle \mathbf{f}_{\alpha m}\Big|\mathbf{\Gamma}^{\rm EM}(\mathbf{A})+\mathbf{\Gamma}^{\rm EM}(\mathbf{B})\Big|\mathbf{f}_{\beta n}\Big\rangle \\ &= -ik^{\rm A}\Big\langle \mathbf{f}_{\alpha m}\Big|\mathbf{C}(k^{\rm A})\Big|\mathbf{f}_{\beta n}\Big\rangle - ik^{\rm B}\Big\langle \mathbf{f}_{\alpha m}\Big|\mathbf{C}(k^{\rm B})\Big|\mathbf{f}_{\beta n}\Big\rangle \\ M\Big(\mathcal{I}^N_{\alpha m},\mathcal{I}^K_{\beta n}\Big) &= \Big\langle \mathbf{f}_{\alpha m}\Big|\mathbf{\Gamma}^{\rm ME}(\mathbf{A})+\mathbf{\Gamma}^{\rm ME}(\mathbf{B})\Big|\mathbf{f}_{\beta n}\Big\rangle \\ &= -ik^{\rm A}\Big\langle \mathbf{f}_{\alpha m}\Big|\mathbf{C}(k^{\rm A})\Big|\mathbf{f}_{\beta n}\Big\rangle - ik^{\rm B}\Big\langle \mathbf{f}_{\alpha m}\Big|\mathbf{C}(k^{\rm B})\Big|\mathbf{f}_{\beta n}\Big\rangle \\ M\Big(\mathcal{I}^N_{\alpha m},\mathcal{I}^N_{\beta n}\Big) &= -\Big\langle \mathbf{f}_{\alpha m}\Big|\mathbf{\Gamma}^{\rm MM}(\mathbf{A})+\mathbf{\Gamma}^{\rm MM}(\mathbf{B})\Big|\mathbf{f}_{\beta n}\Big\rangle \\ &= -\frac{ik^{\rm A}}{Z^{\rm A}}\Big\langle \mathbf{f}_{\alpha m}\Big|\mathbf{G}(k^{\rm A})\Big|\mathbf{f}_{\beta n}\Big\rangle - \frac{ik^{\rm B}}{Z^{\rm B}}\Big\langle \mathbf{f}_{\alpha m}\Big|\mathbf{G}(k^{\rm B})\Big|\mathbf{f}_{\beta n}\Big\rangle. \end{aligned}$$

9 Evaluation of 2D Integrals over RWG Basis Functions

The **E** and **H** fields due to an electric current distribution described by a single unit-strength RWG basis function $\mathbf{f}_a(\mathbf{x})$ are

$$\mathbf{E}(\mathbf{x}) = ikZ\Big\langle \mathbf{G}(\mathbf{x},\mathbf{x}')\Big|\mathbf{f}_a(\mathbf{x}')\Big\rangle \tag{28}$$

$$\mathbf{H}(\mathbf{x}) = -ik\Big\langle \mathbf{C}(\mathbf{x},\mathbf{x}')\Big|\mathbf{f}_a(\mathbf{x}')\Big\rangle. \tag{29}$$

The fields of a *magnetic* current distribution described by the same basis function are

$$\mathbf{E}(\mathbf{x}) = +ik\Big\langle \mathbf{C}(\mathbf{x},\mathbf{x}')\Big|\mathbf{f}_a(\mathbf{x}')\Big\rangle \tag{30}$$

$$\mathbf{H}(\mathbf{x}) = \frac{ik}{Z}\Big\langle \mathbf{C}(\mathbf{x},\mathbf{x}')\Big|\mathbf{f}_a(\mathbf{x}')\Big\rangle. \tag{31}$$

10 Evaluation of 4D Integrals over RWG Basis Functions

As demonstrated above, the elements of the BEM matrix involve integrals over pairs of RWG basis functions of the form

$$\left\langle \mathbf{f}_a \middle| \mathbf{G}(k) \middle| \mathbf{f}_b \right\rangle \equiv \int_{\sup \mathbf{f}_a} d\mathbf{x}_a \int_{\sup \mathbf{f}_b} d\mathbf{x}_b \, \mathbf{f}_a(\mathbf{x}_a) \cdot \mathbf{G}(k, \mathbf{x}_a - \mathbf{x}_b) \cdot \mathbf{f}_b(\mathbf{x}_b) \tag{32a}$$

$$\left\langle \mathbf{f}_a \middle| \mathbf{C}(k) \middle| \mathbf{f}_b \right\rangle \equiv \int_{\sup \mathbf{f}_a} d\mathbf{x}_a \int_{\sup \mathbf{f}_b} d\mathbf{x}_b \, \mathbf{f}_a(\mathbf{x}_a) \cdot \mathbf{C}(k, \mathbf{x}_a - \mathbf{x}_b) \cdot \mathbf{f}_b(\mathbf{x}_b). \tag{32b}$$

LIBSCUFF computes these integrals using one of two strategies depending on how far apart the basis functions are from one another. To quantify this, let d_{ab} be the distance between the centroids of basis functions $\mathbf{f}_a$ and $\mathbf{f}_b$, and let $R_{\rm max} = \texttt{max}(R_a, R_b)$ be the larger of the radii of the two basis functions. (The "radius" of a compact source distribution is the radius of the smallest sphere in which the source distribution may be enclosed. For RWG basis functions, we take the centroid to be the midpoint of the common edge shared by the two triangle that define the basis function; then the radius is the greatest distance from the centroid to any of the four panel vertices (Figure **??**).)

Then the computation of the integrals (32) proceeds as follows.

1. When $d_{ab} > \texttt{DBFTHRESHOLD} \cdot R_{\rm max}$, we approximate (32) using a spherical-multipole expansion. (Here `DBFThreshold`, the "distant basis-function threshold," is a dimensionless number that must be tuned to yield optimal accuracy and performance; in LIBSCUFF its value is set to 8.3.)

2. Otherwise, we compute (32) as a sum of four numerically-evaluated integrals over pairs of triangular panels.

Each of these methods is described in the following sections.

10.1 Matrix elements between distant basis functions: spherical multipole method

The spherical multipole method is based on the spherical-multipole expansion of the **G** and **C** dyadics:

$$\mathbf{G}(\mathbf{x}, \mathbf{x}') = -ik \sum_\alpha \left\{ \hat{\mathbf{M}}_\alpha(\hat{\mathbf{x}}) \check{\mathbf{M}}^*(\check{\mathbf{x}}) - \hat{\mathbf{N}}_\alpha(\hat{\mathbf{x}}) \check{\mathbf{N}}^*(\check{\mathbf{x}}) \right\}$$

$$\mathbf{C}(\mathbf{x}, \mathbf{x}') = -ik \sum_\alpha \left\{ \hat{\mathbf{M}}_\alpha(\hat{\mathbf{x}}) \check{\mathbf{N}}^*(\check{\mathbf{x}}) + \hat{\mathbf{N}}_\alpha(\hat{\mathbf{x}}) \check{\mathbf{M}}^*(\check{\mathbf{x}}) \right\}$$

where $\hat{\mathbf{x}}(\check{\mathbf{x}})$ denote whichever of $\mathbf{x}, \mathbf{x}'$ is closer to (further from) the origin. (My notation and conventions for spherical multipole functions are summarized in Appendix **??**; briefly, the $\wedge$ adornment means "interior," while $\vee$ means

"exterior," and the mnemonic is to think of $\vee$ as indicating radiation outward to infinity, as is appropriate for exterior solutions).

Inserting into (32), we have

$$\big\langle \mathbf{f}_a \big| \mathbf{G} \big| \mathbf{f}_b \big\rangle = -ik \sum_\alpha \Big\{ \big\langle \mathbf{f}_a \big| \hat{\mathbf{M}}_\alpha \big\rangle \big\langle \check{\mathbf{M}}^*_\alpha \big| \mathbf{f}_b \big\rangle - \big\langle \mathbf{f}_a \big| \hat{\mathbf{N}}_\alpha \big\rangle \big\langle \check{\mathbf{N}}^*_\alpha \big| \mathbf{f}_b \big\rangle \Big\}$$

$$\big\langle \mathbf{f}_a \big| \mathbf{C} \big| \mathbf{f}_b \big\rangle = -ik \sum_\alpha \Big\{ \big\langle \mathbf{f}_a \big| \hat{\mathbf{M}}_\alpha \big\rangle \big\langle \check{\mathbf{N}}^*_\alpha \big| \mathbf{f}_b \big\rangle + \big\langle \mathbf{f}_a \big| \hat{\mathbf{N}}_\alpha \big\rangle \big\langle \check{\mathbf{M}}^*_\alpha \big| \mathbf{f}_b \big\rangle \Big\}$$

Now use the translation matrices [Appendix **??**, equation (**??**)] to rewrite inner products involving exterior functions in terms of inner products involving interior functions:

$$\big\langle \mathbf{f}_a \big| \mathbf{G} \big| \mathbf{f}_b \big\rangle = -ik \sum_{\alpha\beta} \begin{pmatrix} \mathcal{M}_{a\alpha} \\ \mathcal{N}_{a\alpha} \end{pmatrix}^T \begin{pmatrix} A_{\alpha\beta} & B_{\alpha\beta} \\ B_{\alpha\beta} & -A_{\alpha\beta} \end{pmatrix} \begin{pmatrix} \mathcal{M}_{b\alpha} \\ \mathcal{N}_{b\alpha} \end{pmatrix} \tag{33a}$$

$$\big\langle \mathbf{f}_a \big| \mathbf{C} \big| \mathbf{f}_b \big\rangle = -ik \sum_{\alpha\beta} \begin{pmatrix} \mathcal{M}_{a\alpha} \\ \mathcal{N}_{a\alpha} \end{pmatrix}^T \begin{pmatrix} -B_{\alpha\beta} & A_{\alpha\beta} \\ A_{\alpha\beta} & B_{\alpha\beta} \end{pmatrix} \begin{pmatrix} \mathcal{M}_{b\alpha} \\ \mathcal{N}_{b\alpha} \end{pmatrix} \tag{33b}$$

where $\{\mathcal{M}, \mathcal{N}\}$ are the spherical multipole moments of the RWG basis functions:

$$\mathcal{M}_{a\alpha} = \int_{\sup \mathbf{f}_a} \mathbf{f}_a(\mathbf{x}) \cdot \hat{\mathbf{M}}_\alpha(\mathbf{x})\, d\mathbf{x}, \qquad \mathcal{N}_{a\alpha} = \int_{\sup \mathbf{f}_a} \mathbf{f}_a(\mathbf{x}) \cdot \hat{\mathbf{N}}_\alpha(\mathbf{x})\, d\mathbf{x}. \tag{34}$$

The point of this decomposition is that computing the integrals (34) at a given frequency requires $O(\texttt{NBF})$ numerical cubatures, in contrast to the $O(\texttt{NBF}^2)$ numerical cubatures that would naïvely be required to evaluate (32) for all pairs of basis functions.

10.2 Matrix elements between nearby basis functions: panel-panel integration method

When the supports of the basis functions $\mathbf{f}_a$ and $\mathbf{f}_b$ are relatively close to each other, we evaluate each of the integrals in (32) as a sum of four integrals over pairs of triangular panels:

$$\Big\langle \mathbf{f}_a \Big| \mathbf{G}(k) \Big| \mathbf{f}_b \Big\rangle = l_a l_b \sum_{\sigma,\tau=-}^{+} \frac{\sigma\tau}{4A_a^\sigma A_b^\tau} \int_{\mathcal{P}_a^\sigma} d\mathbf{x}_a \int_{\mathcal{P}_b^\tau} d\mathbf{x}_b \Big[h_\bullet(\mathbf{x}_a, \mathbf{x}_b) - \frac{1}{k^2} h_\nabla(\mathbf{x}_a, \mathbf{x}_b) \Big] \phi\big(k, |\mathbf{x}_a - \mathbf{x}_b|\big) \tag{35a}$$

$$\Big\langle \mathbf{f}_a \Big| \mathbf{C}(k) \Big| \mathbf{f}_b \Big\rangle = \frac{l_a l_b}{ik} \sum_{\sigma,\tau=-}^{+} \frac{\sigma\tau}{4A_a^\sigma A_b^\tau} \int_{\mathcal{P}_a^\sigma} d\mathbf{x}_a \int_{\mathcal{P}_b^\tau} d\mathbf{x}_b\, h_\times(\mathbf{x}_a, \mathbf{x}_b) \psi\big(k, |\mathbf{x}_a - \mathbf{x}_b|\big) \tag{35b}$$

where[7]

$$\begin{aligned}
h_\bullet(\mathbf{x}_a,\mathbf{x}_b) &= (\mathbf{x}_a-\mathbf{Q}_a)\cdot(\mathbf{x}_b-\mathbf{Q}_b)\\
h_\nabla(\mathbf{x}_a,\mathbf{x}_b) &= 4\\
h_\times(\mathbf{x}_a,\mathbf{x}_b) &= \Big[(\mathbf{x}_a-\mathbf{Q}_a)\times(\mathbf{x}_b-\mathbf{Q}_b)\Big]\cdot(\mathbf{x}_a-\mathbf{x}_b)\\
&= (\mathbf{x}_a\times\mathbf{x}_b)\cdot(\mathbf{Q}_a-\mathbf{Q}_b)+(\mathbf{Q}_a\times\mathbf{Q}_b)\cdot(\mathbf{x}_a-\mathbf{x}_b)\\
\phi(k,r) &= \frac{e^{ikr}}{4\pi r},\\
\psi(k,r) &= (ikr-1)\frac{e^{ikr}}{4\pi r^3}.
\end{aligned}$$

[Note that ψ is defined such that $\nabla\phi(k,|\mathbf{r}|)=\mathbf{r}\psi(k,|\mathbf{r}|)$].

The point of this notation is that it expresses the integrands of the panel-panel integrals in (35) as products of benign polynomials in $\mathbf{x}_a,\mathbf{x}_b$ (the h functions) times kernel functions that depend only on the distance $\mathbf{x}_a-\mathbf{x}_b$ and have singularities when this distance vanishes (the ϕ,ψ kernels). This decomposition facilitates the desingularization procedure described below.

In some cases I will write (35) using the notation

$$\Big\langle \mathbf{f}_a\Big|\mathbf{G}(k)\Big|\mathbf{f}_b\Big\rangle = l_a l_b \sum_{\sigma,\tau=-}^{+}\sigma\tau\left\{\texttt{PPI}\Big(\mathcal{P}_a^\sigma,\mathcal{P}_b^\tau,h_\bullet,\phi\Big)-\frac{1}{k^2}\texttt{PPI}\Big(\mathcal{P}_a^\sigma,\mathcal{P}_b^\tau,h_\nabla,\phi\Big)\right\} \tag{36a}$$

$$\Big\langle \mathbf{f}_a\Big|\mathbf{C}(k)\Big|\mathbf{f}_b\Big\rangle = \frac{l_a l_b}{ik}\sum_{\sigma,\tau=-}^{+}\sigma\tau\cdot\texttt{PPI}\Big(\mathcal{P}_a^\sigma,\mathcal{P}_b^\tau,h_\times,\psi\Big) \tag{36b}$$

with the "panel-panel integral" functions defined by

$$\texttt{PPI}\Big(\mathcal{P},\mathcal{P}',h,g\Big)\equiv\frac{1}{4AA'}\int_{\mathcal{P}}d\mathbf{x}\int_{\mathcal{P}'}d\mathbf{x}'\,h(\mathbf{x},\mathbf{x}')\,g(|\mathbf{x}-\mathbf{x}'|). \tag{37}$$

The quantities (37) are what are computed by the `GetPanelPanelInteractions()` routine in LIBSCUFF. The responsibility of assembling these quantities together with the requisite prefactors to obtain the full inner products (36) is handled by the routine `GetEdgeEdgeInteractions()`.

Evaluation of distant panel-panel integrals: Cubature

When the panels $\mathcal{P},\mathcal{P}'$ in (37) are relative far away from each other, we evaluate the four-dimensional integral using numerical cubature. For this purpose it is convenient to parameterize points in the triangles using the prescription (Figure **??**)

$$\begin{aligned}
\mathbf{x} &= \mathbf{V}_1+u\mathbf{A}+v\mathbf{B}, \qquad 0\le u\le 1, \quad 0\le v\le u\\
\mathbf{x}' &= \mathbf{V}_1'+u'\mathbf{A}'+v'\mathbf{B}' \quad 0\le u'\le 1, \quad 0\le v'\le u'.
\end{aligned} \tag{38}$$

[7] *Warning:* My notation for the h functions hides the fact that $h_\bullet$ and $h_\times$ depend on the current source/sink nodes $\mathbf{Q}_{ab}^{\pm}$ within the two triangles.

The integral (37) becomes

$$\texttt{PPI}\Big(\mathcal{P},\mathcal{P}',h,g\Big) = \int_0^1 du \int_0^u dv \int_0^1 du' \int_0^{u'} dv'\, h(u,v,u',v')g(u,v,u',v') \tag{39}$$

where the prefactor $\frac{1}{4AA'}$ is cancelled by the Jacobian of the variable transformation (38), and where I put

$$h(u,v,u',v') = h\Big(\mathbf{x}(u,v),\mathbf{x}'(u',v')\Big), \qquad g(u,v,u',v') = g\Big(|\mathbf{x}(u,v)-\mathbf{x}'(u',v')|\Big).$$

The integral (39) may be evaluated numerically in one of two ways:

1. by nesting two cubature rules for the standard triangle with vertices $\{(0,0),(0,1),(1,0)\}$, or
2. by mapping the domain of integration to the four-dimensional hypercube $[0,1]\times[0,1]\times[0,1]\times[0,1]$ and using a four-dimensional cubature rule for this hypercube. (The variable transformation that enables this mapping is
$$v = ut, \qquad dv = udt, \qquad \int_0^u f(v)dv = \int_0^1 uf(ut)dt$$
and similarly $v' = u't'$.)

The former of these two strategies is slightly more efficient, but the latter has the advantage of allowing the use of standard codes for adaptive cubature over hypercubes.[8] Both strategies are used in LIBSCUFF.

Evaluation of nearby panel-panel integrals: Desingularization

When the panels in (37) have one or more common vertices, the integrand becomes singular at one or more points in the domain of integration. Although these are *integrable* singularities, their existence precludes application of the naïve numerical cubature scheme discussed above, and instead we must resort to more complicated, and more costly, numerical methods.

On the other hand, when the panels have no common vertices but are nearby one another, the integrand in (37) is nonsingular but rapidly varying over the domain of integration, and evaluation of the integral by numerical cubature is technically possible but expensive due to the large number of cubature points required to obtain decent accuracy.

$$\iint h\phi = \iint h\phi^{\rm DS} + \sum_{n=0}^{3} \frac{(ik)^n}{4\pi} A_n \iint hr^{n-1} \tag{40a}$$

$$\iint h\psi = \iint h\psi^{\rm DS} + \sum_{n=0}^{4} \frac{(ik)^n}{4\pi} B_n \iint hr^{n-3} \tag{40b}$$

Here we are using a shorthand in which

[8] `http://ab-initio.mit.edu/cubature`

- h is any of the functions $\{h_\bullet, h_\triangledown, h_\times\}$,
- $\int\!\!\int$ is shorthand for $\int_{\mathcal{P}_a} d\mathbf{x}_a \int_{\mathcal{P}_b} d\mathbf{x}_b$,
- $\int\!\!\int hr^p$ is shorthand for $\int_{\mathcal{P}_a} d\mathbf{x}_a \int_{\mathcal{P}_b} d\mathbf{x}_b \left\{h(\mathbf{x}_a,\mathbf{x}_b)|\mathbf{x}_a-\mathbf{x}_b|^p\right\}$,
- the A coefficients in (40a) are

$$A_n = \frac{1}{n!}$$

- the B coefficients in (40b) are

$$B_0 = -1, \qquad B_1 = 0, \qquad B_2 = \frac{1}{2}, \qquad B_3 = \frac{1}{3}, \qquad B_4 = \frac{1}{6}$$

- the desingularized kernels are

$$\begin{aligned}\phi^{\rm DS}(k,r) &= \frac{e^{ikr} - 1 - ikr - \frac{1}{2}(ikr)^2 - \frac{1}{6}(ikr)^3}{4\pi r}, \\ &\equiv \frac{\texttt{ExpRel}(ikr,4)}{4\pi r} \end{aligned} \tag{41a}$$

  and similarly

$$\psi^{\rm DS}(k,r) \equiv (ikr-1)\frac{\texttt{ExpRel}(ikr,4)}{4\pi r^3}. \tag{41b}$$

When computing the "relative exponential" functions $\texttt{ExpRel}(x,n)$ in (41) it is important that we *not* simply compute `exp(x)` and then subtract off the first n terms in its Taylor series, as doing so could lead to catastrophic loss of numerical precision. Instead, a better-behaved procedure is simply to sum the Taylor series for the exponential starting with its $(n+1)$th term.

11 Evaluation of Frequency-Independent Panel-Panel Integrals

The frequency-independent panel-panel integrals (FIPPIs) are

$$\iint h_\bullet r^p, \qquad \iint h_\nabla r^p, \qquad \iint h_\times r^p \tag{42}$$

where $\iint$ denotes the four-dimensional integration over the pair of triangles as in the previous section.

Evaluation of $\iint h_\bullet r^p$

In terms of the u, v, u', v' variables of equation (38), we have

$$h_\bullet(u,v,u',v') = \Big[\big(\mathbf{V}_1 - \mathbf{Q}\big) + u\mathbf{A} + v\mathbf{B}\Big] \cdot \Big[\big(\mathbf{V}_1' - \mathbf{Q}'\big) + u'\mathbf{A}' + v'\mathbf{B}'\Big] \tag{43}$$

and

$$r(u,v,u',v') = \Big|\mathbf{V}_1 - \mathbf{V}_1' + u\mathbf{A} + v\mathbf{B} - u'\mathbf{A}' - v'\mathbf{B}'\Big|.$$

Expanding the product (43) yields a sum of nine terms:

$$\begin{aligned}\iint h_\bullet r^p = \big(\mathbf{V}_1 - \mathbf{Q}\big)\cdot\big(\mathbf{V}_1' - \mathbf{Q}'\big)\cdot \iint r^p \\ +\mathbf{A}\cdot\big(\mathbf{V}_1' - \mathbf{Q}'\big)\iint ur^p \\ +\mathbf{B}\cdot\big(\mathbf{V}_1' - \mathbf{Q}'\big)\iint vr^p \\ +\cdots \\ +\mathbf{B}\cdot\mathbf{B}'\iint vv'r^p.\end{aligned} \tag{44}$$

It is important to notice that the integrals in (44) are independent of $\mathbf{Q}$ and $\mathbf{Q}'$. This suggests that, to compute $\iint h_\bullet r^p$, I first compute the quantities

$$\iint \left\{ \begin{array}{c} 1 \\ u \\ v \\ u' \\ uu' \\ vu' \\ v' \\ uv' \\ vv' \end{array} \right\} r^p \tag{45}$$

and then use (44) to compute $\iint h_\bullet r^p$. The point of this step is that the quantities (45) need only be evaluated and stored once for each pair of panels, after which the results may be used in (44) to compute the nine separate quantities $\iint h_\bullet r^p$ that result different choices of the current source/sink vertices $\mathbf{Q}, \mathbf{Q}'$.

The integrals (44) are known in LIBSCUFF as the "**Q**-independent FIPPIs," while (42) are the "**Q**-dependent FIPPIs."

Evaluation of $\iint h_\nabla r^p$

Once we have evaluated the **Q**-independent FIPPIs for a pair of panels, we get $\iint h_\nabla r^p$ for free, since it is just the first entry in equation (45) times 4.

Evaluation of $\iint h_\times r^p$

For $p > -3$, I proceed in analogy to equation (44) by writing $h_\times$ as a sum of nine terms,

$$h_\times = \sum_{abcd} u^a v^b u'^c v'^d h_\times^{abcd},$$

whereupon $\iint h_\times r^p$ may be reconstructed from the QIFIPPIs (45) according to

$$\iint h_\times r^p = \sum_{abcd} h_\times^{abcd} \iint \Big[u^a v^b u'^c v'^d\Big] r^p. \tag{46}$$

The nonzero values of $h_\times^{abcd}$ are

$$\begin{aligned}
h_\times^{0000} &= (\mathbf{Q}_a \times \mathbf{Q}_b)\cdot(\mathbf{V}_0 - \mathbf{V}_0') + (\mathbf{Q}_a - \mathbf{Q}_b)\cdot(\mathbf{V}_0 \times \mathbf{V}_0') \\
h_\times^{1000} &= (\mathbf{Q}_a \times \mathbf{Q}_b)\cdot\mathbf{A} + (\mathbf{Q}_a - \mathbf{Q}_b)\cdot(\mathbf{A} \times \mathbf{V}_0') \\
h_\times^{0100} &= (\mathbf{Q}_a \times \mathbf{Q}_b)\cdot\mathbf{B} + (\mathbf{Q}_a - \mathbf{Q}_b)\cdot(\mathbf{B} \times \mathbf{V}_0') \\
h_\times^{0010} &= -(\mathbf{Q}_a \times \mathbf{Q}_b)\cdot\mathbf{A}' + (\mathbf{Q}_a - \mathbf{Q}_b)\cdot(\mathbf{V}_0 \times \mathbf{A}') \\
h_\times^{0001} &= -(\mathbf{Q}_a \times \mathbf{Q}_b)\cdot\mathbf{B}' + (\mathbf{Q}_a - \mathbf{Q}_b)\cdot(\mathbf{V}_0 \times \mathbf{B}') \\
h_\times^{1010} &= (\mathbf{Q}_a - \mathbf{Q}_b)\cdot(\mathbf{A} \times \mathbf{A}') \\
h_\times^{1001} &= (\mathbf{Q}_a - \mathbf{Q}_b)\cdot(\mathbf{A} \times \mathbf{B}') \\
h_\times^{0110} &= (\mathbf{Q}_a - \mathbf{Q}_b)\cdot(\mathbf{B} \times \mathbf{A}') \\
h_\times^{0101} &= (\mathbf{Q}_a - \mathbf{Q}_b)\cdot(\mathbf{B} \times \mathbf{B}').
\end{aligned}$$

For the particular case $p = -3$, the above procedure is ill-behaved, and instead I write

$$\iint h_\times r^{-3} = (\mathbf{Q}_a \times \mathbf{Q}_b)\cdot\iint(\mathbf{x}_a - \mathbf{x}_b) r^{-3} + (\mathbf{Q}_a - \mathbf{Q}_b)\cdot\iint(\mathbf{x}_a \times \mathbf{x}_b) r^{-3} \tag{47}$$

where now

$$\iint(\mathbf{x}_a - \mathbf{x}_b) r^{-3}, \qquad \iint(\mathbf{x}_a \times \mathbf{x}_b) r^{-3} \tag{48}$$

are to be included among the list of **Q**−independent FIPPIs that must be calculated for each panel pair.

On first glance, it might seem that equations (45) and (48) are redundant, since knowing the former should allow reconstruction of the latter. This appearance is deceptive, because for panel pairs with common vertices some of the individual FIPPIs (45) are divergent for $p = -3$, while (48) are convergent. [For panel pairs with no common vertices, the integrals (45) are convergent but much more expensive to calculate than (48).] Of course, for $p = -3$ the **Q**−independent FIPPIs defined by (48) are the only ones we *need* (because for $p = -3$ the only **Q**-dependent FIPPI we need is $\iint h_\times r^p$), while for $p > -3$ equation (48) does not suffice and we need instead the full set (45). Thus a reasonable compromise seems to be to compute only (48) for the case $p = -3$, and to compute the full set (45) for $p > -3$.

Evaluation of Q-independent FIPPIs

The **Q**-independent FIPPIs, equation (45), are nominally four-dimensional integrals, but we have the following simplifications:

1. For $p = 0$ the integral may be done analytically in closed form. (Actually, the same is true for $p = 2$, but the result is too cumbersome to be useful.)

2. If the panels have one or more common vertices, we may use the Taylor-Duffy method (Appendix **??**) to perform one or more of the four integrals analytically.

3. Even when the panels have no common vertices, we can always evaluate one of the four integrals analytically, which accelerates numerical evaluation.

We now address each of these points in turn.

1. FIPPIs for $p = 0$. In this case all the FIPPIs are linear combinations of the basic integral

$$\iint u^a v^b (u')^c (v')^d = \frac{1}{(2+a+b)(1+b)(2+c+d)(1+d)}.$$

We have

$$\iint \left\{ \begin{array}{c} 1 \\ u \\ v \\ u' \\ uu' \\ vu' \\ v' \\ uv' \\ vv' \end{array} \right\} r^0 = \left\{ \begin{array}{c} 1/4 \\ 1/6 \\ 1/12 \\ 1/6 \\ 1/9 \\ 1/18 \\ 1/12 \\ 1/18 \\ 1/36 \end{array} \right\}.$$

2. FIPPIs for panels with common vertices. As noted above, for panels with common vertices the Taylor-Duffy method of Appendix (**??**) is available.

3. FIPPIs for panels with no common vertices. As noted above, even when the panels have no common vertices we can always evaluate one of the four integrals analytically to yield a three-dimensional integral. We arbitrarily choose the integral we evaluate to be the v' integral, and to facilitate its evaluation we write

$$\begin{aligned} r(u,v,u',v') &= \Big|\mathbf{V}_1 - \mathbf{V}_1' + u\mathbf{A} + v\mathbf{B} - u'\mathbf{A}' - v'\mathbf{B}'\Big| \\ &= a\sqrt{(v'+v_0')^2 + b^2}, \end{aligned}$$

$$a = |\mathbf{B}'|, \qquad v_0' = -\frac{1}{a^2}\mathbf{B}'\cdot\mathbf{Y}, \qquad b^2 = \frac{1}{a^2}|\mathbf{Y}|^2 - v_0'^2,$$

$$\mathbf{Y} = \mathbf{V}_1 - \mathbf{V}_1' + u\mathbf{A} + v\mathbf{B} - u'\mathbf{A}'.$$

The integrals we need are now

$$\int_{v_0'}^{v_0'+u'} \left\{ \begin{array}{c} 1 \\ v' \end{array} \right\} \Big[v'^2 + b^2\Big]^{-3/2} dv' = \frac{1}{a^3} \left\{ \begin{array}{c} \frac{(u'+v_0')}{b^2 S_2} - \frac{v_0'}{b^2 S_1} \\ \frac{1}{S_1} - \frac{1}{S_2} \end{array} \right\} \tag{49a}$$

$$\int_{v_0'}^{v_0'+u'} \left\{ \begin{array}{c} 1 \\ v' \end{array} \right\} \Big[v'^2 + b^2\Big]^{-1/2} dv' = \frac{1}{a} \left\{ \begin{array}{c} \log\frac{S_2+(u'+v_0')}{S_1+v_0'} \\ S_2 - S_1 \end{array} \right\} \tag{49b}$$

$$\int_{v_0'}^{v_0'+u'} \left\{ \begin{array}{c} 1 \\ v' \end{array} \right\} \Big[v'^2 + b^2\Big]^{1/2} dv' = a \left\{ \begin{array}{c} \frac{b^2}{2}\log\frac{S_2+(u'+v_0')}{S_1+v_0'} + \frac{1}{2}\big[(u'+v_0')S_2 - v_0'S_1\big] \\ \frac{1}{3}(S_2^3 - S_1^3) \end{array} \right\} \tag{49c}$$

$$\int_{v_0'}^{v_0'+u'} \left\{ \begin{array}{c} 1 \\ v' \end{array} \right\} \Big[v'^2 + b^2\Big] dv' = a^2 \left\{ \begin{array}{c} \\ \end{array} \right\} \tag{49d}$$

$$S_1 \equiv \sqrt{b^2 + v_0'^2}, \qquad S_2 \equiv \sqrt{b + (v_0' + u')^2},$$

To make use of these results in evaluating the FIPPIs (45), we eliminate the v' integrals and replace all factors of $\{1, v'\}$ with their counterparts on the RHS of (49), leaving behind three-dimensional integrals that succumb readily to numerical cubature.

12 Derivatives of Matrix Elements

For Casimir computations we need derivatives of matrix elements with respect to rigid displacements and rotations of basis functions.

12.1 Derivatives by Spherical-Multipole Method

12.2 Derivatives by Panel-Panel Integral Method

We write the panel-panel decomposition of the RWG inner products, equation (36), in the form

$$\Big\langle \mathbf{f}_a \Big| \mathbf{G}(k) \Big| \mathbf{f}_b \Big\rangle = l_a l_b \sum_{\sigma,\tau=-}^{+} \sigma\tau \left\{ H_\bullet(\mathcal{P}_a^\sigma, \mathcal{P}_b^\sigma, \mathbf{R}) - \frac{1}{k^2} H_\nabla(\mathcal{P}_a^\sigma, \mathcal{P}_b^\sigma, \mathbf{R}) \right\} \tag{50a}$$

$$\Big\langle \mathbf{f}_a \Big| \mathbf{C}(k) \Big| \mathbf{f}_b \Big\rangle = \frac{l_a l_b}{ik} \sum_{\sigma,\tau=-}^{+} \sigma\tau \cdot H_\times(\mathcal{P}_a^\sigma, \mathcal{P}_b^\sigma, \mathbf{R}) \tag{50b}$$

where

$$H_\bullet(\mathcal{P}_a, \mathcal{P}_b, \mathbf{R}) = \frac{1}{4A_aA_b} \int_{\mathcal{P}_a} d\mathbf{y}_a \int_{\mathcal{P}_b} d\mathbf{y}_b \, h_\bullet(\mathbf{y}_a, \mathbf{y}_b) \phi\big(k, \mathbf{R} + \mathbf{y}_a - \mathbf{y}_b\big) \tag{51a}$$

$$H_\nabla(\mathcal{P}_a, \mathcal{P}_b, \mathbf{R}) = \frac{1}{4A_aA_b} \int_{\mathcal{P}_a} d\mathbf{y}_a \int_{\mathcal{P}_b} d\mathbf{y}_b \, h_\nabla(\mathbf{y}_a, \mathbf{y}_b) \phi\big(k, \mathbf{R} + \mathbf{y}_a - \mathbf{y}_b\big) \tag{51b}$$

$$H_\times(\mathcal{P}_a, \mathcal{P}_b, \mathbf{R}) = \frac{1}{4A_aA_b} \int_{\mathcal{P}_a} d\mathbf{y}_a \int_{\mathcal{P}_b} d\mathbf{y}_b \, h_\times(\mathbf{y}_a, \mathbf{y}_b, \mathbf{R}) \psi\big(k, \mathbf{R} + \mathbf{y}_a - \mathbf{y}_b\big). \tag{51c}$$

Here we have rewritten the integrals over $\mathbf{x}_a, \mathbf{x}_b$ in equation (35) using new integration variables defined relative to the panel centroids (Figure 6):

$$\mathbf{x}_a = \mathbf{x}_{a0} + \mathbf{y}_a, \qquad \mathbf{x}_b = \mathbf{x}_{b0} + \mathbf{y}_b, \qquad \mathbf{R}_{ab} \equiv \mathbf{R} = \mathbf{x}_{a0} - \mathbf{x}_{b0}. \tag{52}$$

(In equation (51), note that $h_\times$, unlike $h_\bullet$ and h_∇, depends on $\mathbf{R}$ in addition to $\mathbf{y}_a, \mathbf{y}_b$.)

Now we can take derivatives with respect to the components of $\mathbf{R}$. Putting $\mathbf{r} = \mathbf{R} + \mathbf{y}_a - \mathbf{y}_b$), we have

$$\begin{aligned}
\frac{\partial H_\bullet}{\partial \mathbf{R}_i} &= \int d\mathbf{y}_a \int d\mathbf{y}_b \, \mathbf{r}_i h_\bullet(\mathbf{y}_a, \mathbf{y}_b) \psi\big(k, \mathbf{R} + \mathbf{y}_a - \mathbf{y}_b\big) \\
\frac{\partial H_\nabla}{\partial \mathbf{R}_i} &= \int d\mathbf{y}_a \int d\mathbf{y}_b \, \mathbf{r}_i h_\nabla(\mathbf{y}_a, \mathbf{y}_b) \psi\big(k, \mathbf{R} + \mathbf{y}_a - \mathbf{y}_b\big) \\
\frac{\partial H_\times}{\partial \mathbf{R}_i} &= \int d\mathbf{y}_a \int d\mathbf{y}_b \, \mathbf{r}_i h_\times(\mathbf{y}_a, \mathbf{y}_b, \mathbf{R}) \zeta\big(k, \mathbf{R} + \mathbf{y}_a - \mathbf{y}_b\big) \\
&\quad + \int d\mathbf{y}_a \int d\mathbf{y}_b \, \frac{\partial h_\times(\mathbf{y}_a, \mathbf{y}_b, \mathbf{R})}{\partial \mathbf{R}_i} \psi\big(k, \mathbf{R} + \mathbf{y}_a - \mathbf{y}_b\big)
\end{aligned}$$

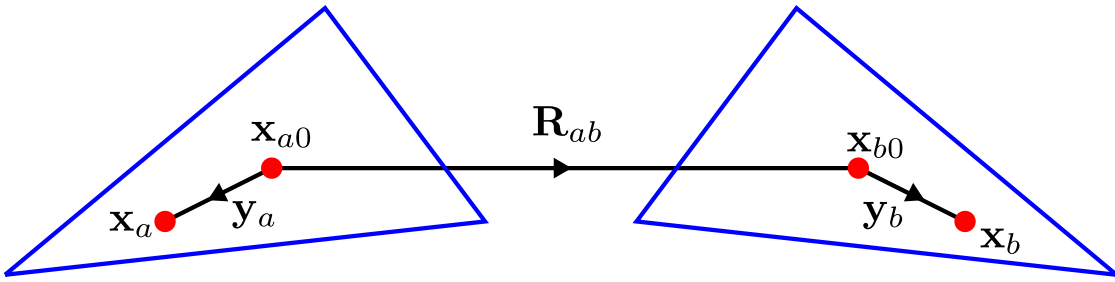

Figure 6: Notation for equation 52.

In the last line, we put

$$\zeta(k,r) = \Big[(ikr)^2 - 3ikr + 3\Big]\frac{e^{ikr}}{4\pi r^5}$$

[which is defined such that $\nabla\psi(k,|\mathbf{r}|) = \mathbf{r}\zeta(k,|\mathbf{r}|)$] and we have

$$\begin{aligned}\frac{\partial h_\times(\mathbf{y}_a,\mathbf{y}_b,\mathbf{R})}{\partial \mathbf{R}_i} &= \frac{\partial}{\partial \mathbf{R}_i}\Big\{\Big[(\mathbf{y}_a-\mathbf{Q}_a)\times(\mathbf{y}_b-\mathbf{Q}_b)\Big]\cdot\mathbf{R}\Big\} \\ &= \Big[(\mathbf{y}_a-\mathbf{Q}_a)\times(\mathbf{y}_b-\mathbf{Q}_b)\Big]_i.\end{aligned}$$

Desingularization

$$\begin{aligned}
\frac{\partial H_\bullet}{\partial \mathbf{R}_i} &= \iint \mathbf{r}_i \mathbf{h}_\bullet \psi \\
&= \iint \mathbf{r}_i h_\bullet \psi^{\text{DS}} + \sum_{n=0}^{4} \frac{(ik)^n}{4\pi} B_n \iint \mathbf{r}_i h_\bullet r^{n-3}
\end{aligned}$$

$$\begin{aligned}
\frac{\partial H_\nabla}{\partial \mathbf{R}_i} &= \iint \mathbf{r}_i h_\nabla \psi \\
&= \left[\iint \mathbf{r}_i h_\nabla \psi^{\text{DS}} + \sum_{n=0}^{4} \frac{(ik)^n}{4\pi} B_n \iint \mathbf{r}_i h_\nabla r^{n-3} \right]
\end{aligned}$$

$$\begin{aligned}
\frac{\partial H_\times}{\partial \mathbf{R}_i} &= \iint \mathbf{r}_i h_\times \zeta + \iint \left(\frac{\partial h_\times}{\partial \mathbf{R}_i} \right) \psi \\
&= \iint \mathbf{r}_i h_\times \zeta^{\text{DS}} + \iint \left(\frac{\partial h_\times}{\partial \mathbf{R}_i} \right) \psi^{\text{DS}} \\
&\quad + \left[\sum_{n=0}^{5} \frac{(ik)^n}{4\pi} C_n \iint \mathbf{r}_i h_\times r^{n-5} \right] + \left[\sum_{n=0}^{4} \frac{(ik)^n}{4\pi} B_n \iint \left(\frac{\partial h_\times}{\partial \mathbf{R}_i} \right) r^{n-3} \right]
\end{aligned}$$

In the last line here we used

$$\zeta^{\text{DS}}(k,r) = \Big[(ikr)^2 - 3ikr + 3 \Big] \frac{\texttt{ExpRel(ikr,4)}}{4\pi r^5}$$

and the C_n coefficients are

$$C_0 = 3, \qquad C_1 = 0, \qquad C_2 = -\frac{1}{2}, \qquad C_3 = C_4 = 0, \qquad C_5 = \frac{1}{6}.$$

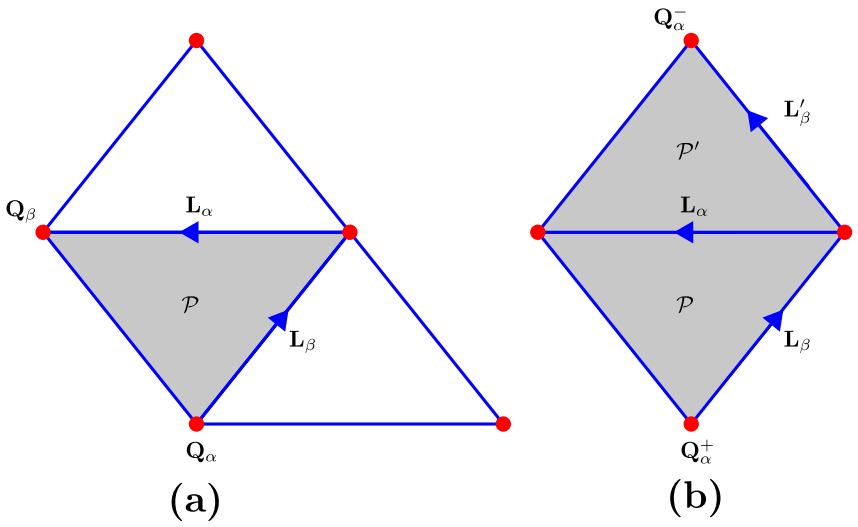

Figure 7: Notation for computation of overlap integrals.

13 Other Panel Integrals

13.1 Overlap Integral

The overlap integral between two RWG basis functions is

$$O_{\alpha\beta} = \left\langle \mathbf{f}_\alpha \middle| \mathbf{f}_\beta \right\rangle = \int_{\sup \mathbf{f}_\alpha \cap \sup \mathbf{f}_\beta} \mathbf{f}_\alpha(\mathbf{x}) \cdot \mathbf{f}_\beta(\mathbf{x})\, d\mathbf{x}.$$

If we think of $O_{\alpha\beta}$ as the α, β element of a matrix $\mathbf{O}$, then $\mathbf{O}$ is a very sparse matrix, with at most 5 nonzero entries per row. Fix an interior edge $\mathbf{L}_\alpha$ in a triangular surface mesh and consider the basis function $\mathbf{f}_\alpha$ associated with this edge. The only basis functions to have nonvanishing overlap with $\mathbf{f}_\alpha$ are **(1)** $\mathbf{f}_\alpha$ itself, and **(2)** basis functions associated with the four edges beside $\mathbf{L}_\alpha$ on the two panels that share $\mathbf{L}_\alpha$, such as $\mathbf{L}_\beta$ in Figure 7**(a)**.

The case $\alpha \neq \beta$. Consider first the case of inequal basis functions $\mathbf{f}_\alpha, \mathbf{f}_\beta$ that share a single panel $\mathcal{P}$ [Figure 7**(a)**]. We parameterize points within $\mathcal{P}$ according to

$$\mathbf{x} = \mathbf{Q}_\alpha + u\mathbf{L}_\beta + v\mathbf{L}_\alpha, \qquad 0 \le u \le 1, \quad 0 \le v \le u.$$

On $\mathcal{P}$, the two basis functions may be expressed in terms of this parameterization as

$$\begin{aligned}\mathbf{f}_\alpha(\mathbf{x}) &= \frac{\sigma^\alpha l_\alpha}{2A}\Big[u\mathbf{L}_\beta + v\mathbf{L}_\alpha\Big] \\ \mathbf{f}_\beta(\mathbf{x}) &= \frac{\sigma^\beta l_\beta}{2A}\Big[u\mathbf{L}_\beta + v\mathbf{L}_\alpha + (\mathbf{Q}_\alpha - \mathbf{Q}_\beta)\Big] \\ &= \frac{\sigma^\beta l_\beta}{2A}\Big[(u-1)\mathbf{L}_\beta + (v-1)\mathbf{L}_\alpha\Big]\end{aligned}$$

Here A is the area of $\mathcal{P}$ and $\sigma^\alpha = \pm 1$ according as $\mathcal{P}$ is the positive or negative panel associated with basis function $\mathbf{f}_\alpha$ (and similarly for σ^β), and we used the fact that $\mathbf{Q}_\alpha + \mathbf{L}_\beta + \mathbf{L}_\alpha = \mathbf{Q}_\beta$.

The overlap integral is

$$\begin{aligned}O_{\alpha\beta} &= \int_{\mathcal{P}} \mathbf{f}_\alpha(\mathbf{x}) \cdot \mathbf{f}_\beta(\mathbf{x})\, d\mathbf{x} \\ &= \frac{\sigma^\alpha\sigma^\beta l_\alpha l_\beta}{2A}\int_0^1 du \int_0^u dv \Big[u\mathbf{L}_\beta + v\mathbf{L}_\alpha\Big]\cdot\Big[(u-1)\mathbf{L}_\beta + (v-1)\mathbf{L}_\alpha\Big] \\ &= -\frac{\sigma^\alpha\sigma^\beta l_\alpha l_\beta}{24A}\Big[l_\alpha^2 + l_\beta^2 + 3\mathbf{L}_\alpha\cdot\mathbf{L}_\beta\Big] \qquad (53)\end{aligned}$$

The case $\alpha = \beta$. In this case there are two panels that contribute [Figure 7**(b)**]. The contribution of $\mathcal{P}$ is

$$\begin{aligned}\int_{\mathcal{P}} \mathbf{f}_\alpha(\mathbf{x})\cdot\mathbf{f}_\alpha(\mathbf{x})\, d\mathbf{x} &= \frac{l_\alpha^2}{2A}\int_0^1 du\int_0^u dv\Big[u\mathbf{L}_\beta + v\mathbf{L}_\alpha\Big]\cdot\Big[u\mathbf{L}_\beta + v\mathbf{L}_\alpha\Big] \\ &= \frac{l_\alpha^2}{24A}\Big[3l_\alpha^2 + l_\beta^2 + 3\mathbf{L}_\alpha\cdot\mathbf{L}_\beta\Big].\end{aligned}$$

Adding the contribution of $\mathcal{P}'$, the total overlap integral is

$$O_{\alpha\alpha} = \frac{l_\alpha^2}{24}\left\{\frac{1}{A}\Big[l_\alpha^2 + 3l_\beta^2 + 3\mathbf{L}_\alpha\cdot\mathbf{L}_\beta\Big] + \frac{1}{A'}\Big[l_\alpha^2 + 3l_\beta'^2 + 3\mathbf{L}_\alpha\cdot\mathbf{L}'_\beta\Big]\right\}. \qquad (54)$$

13.2 Crossed Overlap Integral

The crossed overlap integral between two RWG basis functions is

$$O^\times_{\alpha\beta} = \Big\langle \mathbf{f}_\alpha \Big| \hat{\mathbf{n}}\times\mathbf{f}_\beta\Big\rangle = \int_{\sup\,\mathbf{f}_\alpha\,\cap\,\sup\,\mathbf{f}_\beta} \mathbf{f}_\alpha(\mathbf{x})\cdot\Big[\hat{\mathbf{n}}(\mathbf{x})\times\mathbf{f}_\beta(\mathbf{x})\Big]\, d\mathbf{x}$$

where $\hat{\mathbf{n}}(\mathbf{x})$ is the surface normal at $\mathbf{x}$. (The direction of $\hat{\mathbf{n}}$ must be chosen consistently; in LIBSCUFF this is done by placing one or more *reference points* inside closed objects and choosing the surface normal to each panel to point *away* from the nearest reference point.)

$O^{\times}_{\alpha\beta}$ is only nonzero in the case of Figure 7**(b)**. (In particular, the diagonal element $O^{\times}_{\alpha\alpha}$ vanishes.) Proceeding in analogy to the computation leading to equation (53), we find

$$\begin{aligned}
O^{\times}_{\alpha\beta} &= \int_{\mathcal{P}} \mathbf{f}_\alpha(\mathbf{x}) \cdot \Big[\hat{\mathbf{n}} \times \mathbf{f}_\beta(\mathbf{x})\Big]\, d\mathbf{x} \\
&= \frac{\sigma^\alpha \sigma^\beta l_\alpha l_\beta}{2A} \int_0^1 du \int_0^u dv \Big[u\mathbf{L}_\beta + v\mathbf{L}_\alpha\Big] \cdot \Big[(u-1)\big(\hat{\mathbf{n}} \times \mathbf{L}_\beta\big) + (v-1)\big(\hat{\mathbf{n}} \times \mathbf{L}_\alpha\big)\Big] \\
&= \frac{\sigma^\alpha \sigma^\beta l_\alpha l_\beta}{12A} \Big[\mathbf{L}_\alpha \cdot (\hat{\mathbf{n}} \times \mathbf{L}_\beta)\Big] \\
&= \frac{\sigma^\alpha \sigma^\beta l_\alpha l_\beta}{12A} \Big[\hat{\mathbf{n}} \cdot \big(\mathbf{L}_\beta \times \mathbf{L}_\alpha\big)\Big]
\end{aligned}$$

by cyclic permutation of the triple vector product. But the magnitude of the cross product here is just $\hat{\mathbf{n}}$ times twice the panel area,

$$\begin{aligned}
&= \frac{\sigma^\alpha \sigma^\beta l_\alpha l_\beta}{12A} \Big[\hat{\mathbf{n}} \cdot \big(\pm 2A\, \hat{\mathbf{n}}\big)\Big] \\
&= \pm \frac{\sigma^\alpha \sigma^\beta l_\alpha l_\beta}{6}. \qquad (55)
\end{aligned}$$

The $\pm$ sign is determined as follows: Suppose we start at vertex $\mathbf{Q}_\alpha$ and traverse the vertices of $\mathcal{P}$ by following $\mathbf{L}_\beta$, then $\mathbf{L}_\alpha$. If in so doing we encounter the vertices of $\mathcal{P}$ in the order $(0,1,2)$ or a cyclic permutation thereof, then the $+$ sign holds in (55); otherwise (i.e. if we encounter the vertices in the order $(0,2,1)$ or a cyclic permutation thereof) the $-$ sign holds.

An easy way to determine this sign is to look at the indices within $\mathcal{P}$ of vertices $\mathbf{Q}_\beta$ and $\mathbf{Q}_\alpha$. Call these $I_{\mathcal{P}}(\mathbf{Q}_\beta)$ and $I_{\mathcal{P}}(\mathbf{Q}_\alpha)$, respectively; they are integers defined modulo 3. Then the sign in (55) is

$$\text{sign in equation (55)} = \begin{cases} +, & \text{if } I_{\mathcal{P}}(\mathbf{Q}_\beta) - I_{\mathcal{P}}(\mathbf{Q}_\alpha) \equiv 2 \bmod 3 \\ -, & \text{if } I_{\mathcal{P}}(\mathbf{Q}_\beta) - I_{\mathcal{P}}(\mathbf{Q}_\alpha) \equiv 1 \bmod 3. \end{cases}$$

14 Spherical Multipole Moments

Definition of the Spherical Multipole Moments

Following Jackson and other authors, I define the electric and magnetic spherical multipole moments of a localized source distribution to be the coefficients in a spherical-wave expansion of the fields away from the source regions:

$$\mathbf{E}(\mathbf{r}) = \sum_{\ell m} \Big\{ a^{\rm M}_{\ell,m} \check{\mathcal{M}}_{\ell m}(\mathbf{r}) + a^{\rm E}_{\ell,m} \check{\mathcal{N}}_{\ell m}(\mathbf{r}) \Big\} \tag{56a}$$

$$\mathbf{H}(\mathbf{r}) = \frac{1}{Z} \sum_{\ell m} \Big\{ - a^{\rm M}_{\ell,m} \check{\mathcal{N}}_{\ell m}(\mathbf{r}) + a^{\rm N}_{\ell,m} \check{\mathcal{M}}_{\ell m}(\mathbf{r}) \Big\} \tag{56b}$$

where Z is the wave impedance of the medium ($Z = 377\,\Omega$ for vacuum). Note that my $a^{\rm M}_{\ell,m}, a^{\rm E}_{\ell,m}$ coefficients are not normalized in quite the same way as Jackson's $a_{M}(l,m), a_{E}(l,m)$ coefficients; the relationship is

$$a^{\rm M}_{\ell,m} = Z_0 a_{M}(l,m), \qquad a^{\rm E}_{\ell,m} = Z_0 \frac{i}{k} a_{E}(l,m)$$

Jackson gives expressions (equations 9.167-8) for computing the a coefficients for given source distributions; however, these expressions are not convenient for our purposes.[9] Instead, in the following sections I outline an alternative approach for recovering the a coefficients from known source distributions.

Expansion of the Dyadic Green's Functions in Spherical Helmholtz Solutions

This approach is based on the well-known spherical-wave expansion of the dyadic Green's functions of Section 3. [In the following expression, the ρ and σ subscripts run over spherical vector components $(r,\theta,\phi.)$]

$$G_{\rho\sigma}(k;\mathbf{r}-\mathbf{r}') = \quad ik \sum_{\ell m} \Big\{ \check{\mathcal{M}}_{\ell m\rho}(k,\mathbf{r}_>) \hat{\mathcal{M}}^*_{\ell m\sigma}(k,\mathbf{r}_<) + \check{\mathcal{N}}_{\ell m\rho}(k,\mathbf{r}_>) \hat{\mathcal{N}}^*_{\ell m\sigma}(k,\mathbf{r}_>) \Big\} \tag{57a}$$

$$C_{\rho\sigma}(k;\mathbf{r}-\mathbf{r}') = ik \sum_{\ell m} \Big\{ \check{\mathcal{N}}_{\ell m\rho}(k,\mathbf{r}_>) \hat{\mathcal{M}}^*_{\ell m\sigma}(k,\mathbf{r}_<) - \check{\mathcal{M}}_{\ell m\rho}(k,\mathbf{r}_>) \hat{\mathcal{N}}^*_{\ell m\sigma}(k,\mathbf{r}_>) \Big\} \tag{57b}$$

(Note: The expansion for $\mathbf{C}$ here assumes that $|\mathbf{r}| > |\mathbf{r}'|$. In the opposite case in which $|\mathbf{r}| < |\mathbf{r}'|$, the above expression for $\mathbf{C}$ acquires a minus sign.)

[9] In particular, applying Jackson's expressions directly would require evaluating integrals over the quantity $\nabla\cdot\big[\mathbf{r}\times\mathbf{f}^{\rm RWG}(\mathbf{r})\big]$, which vanishes in the *interior* of an RWG panel but makes nonzero contributions at the *edges*. This complication makes Jackson's expressions somewhat unwieldy in our case, whereas the approach outlined above is computationally straightforward.

Fields due to localized current distributions

Now consider the fields arising from localized surface electric and magnetic current distributions $\mathbf{K}(\mathbf{x})$ and $\mathbf{N}(\mathbf{x})$:

$$\mathbf{E}(\mathbf{r}) = ik \int \Big\{ Z\mathbf{G}(k, \mathbf{r}-\mathbf{r}') \cdot \mathbf{K}(\mathbf{r}') + \mathbf{C}(k, \mathbf{r}-\mathbf{r}') \cdot \mathbf{N}(\mathbf{r}') \Big\} \, d\mathbf{r}'$$
$$\mathbf{H}(\mathbf{r}) = ik \int \Big\{ -\mathbf{C}(k, \mathbf{r}-\mathbf{r}') \cdot \mathbf{K}(\mathbf{r}') + \frac{1}{Z}\mathbf{G}(k, \mathbf{r}-\mathbf{r}') \cdot \mathbf{N}(\mathbf{r}') \Big\} \, d\mathbf{r}'.$$

Insert the expansions (57) and assume that the field evaluation point will always be further from the origin than the source current point:

$$\mathbf{E}(\mathbf{r}) = -k^2 \sum_{\ell m} \Bigg\{ \check{\boldsymbol{\mathcal{M}}}_{\ell m}(\mathbf{r}) \cdot \Big[\Big\langle \hat{\boldsymbol{\mathcal{M}}}_{\ell m} \Big| Z\mathbf{K} \Big\rangle - \Big\langle \hat{\boldsymbol{\mathcal{N}}}_{\ell m} \Big| \mathbf{N} \Big\rangle \Big] + \check{\boldsymbol{\mathcal{N}}}_{\ell m}(\mathbf{r}) \cdot \Big[\Big\langle \hat{\boldsymbol{\mathcal{N}}}_{\ell m} \Big| Z\mathbf{K} \Big\rangle + \Big\langle \hat{\boldsymbol{\mathcal{M}}}_{\ell m} \Big| \mathbf{N} \Big\rangle \Big] \Bigg\}$$

$$\mathbf{H}(\mathbf{r}) = -\frac{k^2}{Z_0} \sum_{\ell m} \Bigg\{ \check{\boldsymbol{\mathcal{M}}}_{\ell m}(\mathbf{r}) \cdot \Big[\Big\langle \hat{\boldsymbol{\mathcal{N}}}_{\ell m} \Big| Z\mathbf{K} \Big\rangle + \Big\langle \hat{\boldsymbol{\mathcal{M}}}_{\ell m} \Big| \mathbf{N} \Big\rangle \Big] + \check{\boldsymbol{\mathcal{N}}}_{\ell m}(\mathbf{r}) \cdot \Big[-\Big\langle \hat{\boldsymbol{\mathcal{M}}}_{\ell m} \Big| Z\mathbf{K} \Big\rangle + \Big\langle \hat{\boldsymbol{\mathcal{N}}}_{\ell m} \Big| \mathbf{N} \Big\rangle \Big] \Bigg\}$$

Comparing (58) with the definitions (56) now allows us to read off the expressions for $a^{\mathrm{E,M}}$ in terms of the source distributions $\mathbf{K}$ and $\mathbf{N}$:

$$a^{\mathrm{M}}_{\ell,m} = -k^2 \Big[\Big\langle \hat{\boldsymbol{\mathcal{M}}}_{\ell m} \Big| Z\mathbf{K} \Big\rangle - \Big\langle \hat{\boldsymbol{\mathcal{N}}}_{\ell m} \Big| \mathbf{N} \Big\rangle \Big] \tag{59a}$$

$$a^{\mathrm{E}}_{\ell,m} = -k^2 \Big[\Big\langle \hat{\boldsymbol{\mathcal{N}}}_{\ell m} \Big| Z\mathbf{K} \Big\rangle + \Big\langle \hat{\boldsymbol{\mathcal{M}}}_{\ell m} \Big| \mathbf{N} \Big\rangle \Big] \tag{59b}$$

15 Evaluation of the fields at panel centroids

It is useful to have expressions for the **E** and **H** fields at the centroids of the triangular panels in the discretization of object surfaces. Of course, the solution of the EFIE or PMCHW equations automatically gives us the *tangential* components of the fields on the object surfaces, but to get the normal components we must do a little more work.

Thus, consider the fields at a point lying a distance z above the centroid of a panel in the direction of the outward-pointing panel normal. Let $\boldsymbol{\rho} = (x, y)$ be the in-plane coordinate vector. The normal **E**−field is given by

$$E_z(z) = \int d\boldsymbol{\rho} \Big\{ \Gamma^{\rm EE}_{zx}(\boldsymbol{\rho}, z) K_x(\boldsymbol{\rho}) + \Gamma^{\rm EE}_{zy}(\boldsymbol{\rho}, z) K_y(\boldsymbol{\rho}) \Big\} + \int d\boldsymbol{\rho} \Big\{ \Gamma^{\rm EM}_{zx}(\boldsymbol{\rho}, z) N_x(\boldsymbol{\rho}) + \Gamma^{\rm EM}_{zy}(\boldsymbol{\rho}, z) N_y(\boldsymbol{\rho}) \Big\}. \tag{60}$$

Anticipating that the final answers will involve the first derivatives of **K** and **N** at the origin (i.e. the panel centroid), I write

$$K_x(\boldsymbol{\rho}) = K_x^{(00)} + xK_x^{(10)} + yK_x^{(01)} + xyK_x^{(11)} + \cdots$$
$$K_y(\boldsymbol{\rho}) = K_y^{(00)} + xK_y^{(10)} + yK_y^{(01)} + xyK_y^{(11)} + \cdots$$

(where $K^{(pq)}$ is short for $|\partial^{p+q} K / \partial^p x \partial^q y|_{\boldsymbol{\rho}=0}$) and similarly for the components of **N**. Also, the components of the Γ tensors that I will need are

$$\Gamma^{\rm EE}_{zx} = ikZzx\big[-3 + 3ikr - (ikr)^2\big] \frac{e^{ikr}}{4\pi(ik)^2 r^5}$$
$$\Gamma^{\rm EE}_{zy} = ikZzy\big[-3 + 3ikr - (ikr)^2\big] \frac{e^{ikr}}{4\pi(ik)^2 r^5}$$
$$\Gamma^{\rm EM}_{zx} = iky\big[-1 + ikr\big] \frac{e^{ikr}}{4\pi(ik) r^3}$$
$$\Gamma^{\rm EM}_{zy} = -ikx\big[-1 + ikr\big] \frac{e^{ikr}}{4\pi(ik) r^3}$$

where $r = \sqrt{\boldsymbol{\rho}^2 + z^2}$ and k, Z are the wavenumber and wave impedance for the medium in question. Now I insert everything into (60) and note that terms linear in x and/or y vanish under the angular portion of the $d\boldsymbol{\rho}$ integration:

$$\int d\boldsymbol{\rho} \left\{ \begin{array}{c} 1 \\ x \\ y \\ x^2 \\ xy \\ y^2 \end{array} \right\} = 2\pi \int \rho d\rho \left\{ \begin{array}{c} 1 \\ 0 \\ 0 \\ \rho^2/2 \\ 0 \\ \rho^2/2 \end{array} \right\}$$

This yields

$$E_z(z) = \frac{Z\big(K_x^{(10)} + K_y^{(01)}\big)}{4ik} \cdot z \cdot \int_0^\infty \rho^3 d\rho \,\big[-3 + 3ikr - (ikr)^2\big]\frac{e^{ikr}}{r^5} + \frac{\big(N_x^{(01)} - N_y^{(10)}\big)}{4} \int_0^\infty \rho^3 d\rho \,\big[-1 + ikr\big]\frac{e^{ikr}}{r^3}.$$

The prefactor in the second term here involves the z component of the curl of the magnetic current, $\nabla \times \mathbf{N}$; but the curl of an RWG basis function vanishes in the interior of the panels on which the function is defined, so this term does not contribute.

On the other hand, the first term here is proportional to $\nabla \cdot \mathbf{K}$. Change integration variables to $r = \sqrt{\rho^2 + z^2},\ r\,dr = \rho\,d\rho$:

$$E_z(z) = \frac{Z\big(\nabla \cdot \mathbf{K}\big)}{4ik} \cdot z \cdot \int_z^\infty dr(r^2 - z^2)\,\big[-3 + 3ikr - (ikr)^2\big]\frac{e^{ikr}}{r^4}$$

The only terms in the integrand that lead to nonvanishing results in the $z \to 0$ limit are those coming from the -3 term in the square brackets:

$$-3z \cdot \int_z^\infty \left[\frac{1}{r^2} - \frac{z^2}{r^4}\right] dr = 3z \cdot \left|\frac{1}{r} - \frac{z^2}{3r^3}\right|_z^\infty = 2$$

and thus

$$\lim_{z\to 0} E_z(z) = \frac{Z(\nabla \cdot \mathbf{K})}{2ik} = \frac{(\nabla \cdot \mathbf{K})}{2i\epsilon\omega} = \frac{\sigma}{2\epsilon} \tag{61}$$

where $\sigma = \frac{1}{i\omega}\nabla \cdot \mathbf{K}$ is the surface charge density at the panel centroid.

Equation (61) is of course just the result we would have predicted on the basis of electrostatic arguments, but it is useful to see here how it follows from our full frequency-dependent formalism.

Meanwhile, an analogous calculation for the magnetic field yields

$$\lim_{z\to 0} H_z(z) = -\frac{(\nabla \cdot \mathbf{N})}{2i\mu\omega}. = -\frac{(\nabla \cdot \mathbf{N})}{2ikZ}. \tag{62}$$

Note the minus sign compared to (61).

16 BEM formulations for PBC bodies

16.1 Scattered field of an infinite PEC surface

Consider the scattered field produced by an induced surface-current density $\mathbf{K}(\mathbf{x})$ on an infinite PEC surface $\mathcal{S}_\infty$:

$$\mathbf{E}^{\rm scat}(\mathbf{x}) = \int_{\mathcal{S}_\infty} \mathbf{\Gamma}^{\rm EE}(\mathbf{x},\mathbf{x}')\cdot\mathbf{K}(\mathbf{x}')d\mathbf{x}' \tag{63}$$

$$= ikZ_0 \int_{\mathcal{S}_\infty} \mathbf{G}(\mathbf{x},\mathbf{x}')\cdot\mathbf{K}(\mathbf{x}')d\mathbf{x}' \tag{64}$$

where $k=\omega/c$ (ω is the angular frequency at which we are working) and Z_0 is the impedance of free space (assume we are in vacuum for now). If we now suppose that

- the surface $\mathcal{S}_\infty$ consists of an infinite lattice of copies of a unit-cell surface $\mathcal{S}_0$ translated through two-dimensional lattice vectors of the form

  $$\mathbf{L} = n_1\mathbf{L}_1 + n_2\mathbf{L}_2 \tag{65}$$

  and

- the surface current respects this periodicity in the Bloch sense, i.e. we have

  $$\mathbf{K}(\mathbf{x}+\mathbf{L}) = e^{i\mathbf{k}_{\rm B}\cdot\mathbf{L}}\,\mathbf{K}(\mathbf{x}) \tag{66}$$

  for some Bloch vector $\mathbf{k}_{\rm B}$

then I can write the scattered field (67) as an integral over just the unit cell:

$$\begin{aligned}\mathbf{E}^{\rm scat}(\mathbf{x}) &= ikZ_0\sum_{\mathbf{L}}\int_{\mathcal{S}_0}\mathbf{G}(\mathbf{x},\mathbf{x}'+\mathbf{L})\cdot\mathbf{K}(\mathbf{x}'+\mathbf{L})\,d\mathbf{x}' \\ &= ikZ_0\int_{\mathcal{S}_0}\underbrace{\left\{\sum_{\mathbf{L}} e^{i\mathbf{k}_{\rm B}\cdot\mathbf{L}}\mathbf{G}(\mathbf{x},\mathbf{x}'+\mathbf{L})\right\}}_{\overline{\mathbf{G}}(\mathbf{x},\mathbf{x}')}\cdot\mathbf{K}(\mathbf{x}')\,d\mathbf{x}' \\ &= ikZ_0\int_{\mathcal{S}_0}\overline{\mathbf{G}}(\mathbf{x},\mathbf{x}')\cdot\mathbf{K}(\mathbf{x}')\,d\mathbf{x}'\end{aligned} \tag{67}$$

where $\overline{\mathbf{G}}$ is the dyadic periodic Green's function, whose properties we now discuss.

16.2 Periodic Green's functions

The dyadic periodic Green's function introduced in (67) is

$$\overline{\mathbf{G}}(\mathbf{x},\mathbf{x}') = \sum_{\mathbf{L}} e^{i\mathbf{k}_{\rm B}\cdot\mathbf{L}}\mathbf{G}(\mathbf{x},\mathbf{x}'+\mathbf{L})$$

$$\overline{\mathbf{G}}(\mathbf{x},\mathbf{x}') = \sum_{\mathbf{L}} e^{i\mathbf{k}_{\rm B}\cdot\mathbf{L}}\mathbf{G}(\mathbf{x}-\mathbf{x}'-\mathbf{L})$$

with cartesian components

$$\begin{aligned}\overline{G}_{ij}(\mathbf{x},\mathbf{x}') &= \sum_{\mathbf{L}} e^{i\mathbf{k}_B\cdot\mathbf{L}} G_{ij}(\mathbf{x}-\mathbf{x}'-\mathbf{L}) \\ &= \sum_{\mathbf{L}} e^{i\mathbf{k}_B\cdot\mathbf{L}} \left[\left(\delta_{ij} + \frac{1}{k^2}\partial_i\partial_j\right) \frac{e^{ik|\mathbf{x}-\mathbf{x}'-\mathbf{L}|}}{4\pi|\mathbf{x}-\mathbf{x}'-\mathbf{L}|} \right]\end{aligned}$$

Interchange differentiation and summation:

$$= \left(\delta_{ij} + \frac{1}{k^2}\partial_i\partial_j\right) \underbrace{\left\{ \sum_{\mathbf{L}} e^{i\mathbf{k}_B\cdot\mathbf{L}} \frac{e^{ik|\mathbf{x}-\mathbf{x}'-\mathbf{L}|}}{4\pi|\mathbf{x}-\mathbf{x}'-\mathbf{L}|} \right\}}_{\overline{G}_0(\mathbf{x}-\mathbf{x}')}$$

where $\overline{G}_0$ is the scalar periodic Green's function. (LIBSCUFF computes $\overline{G}_0$ and its derivatives using Ewald summation together with an interpolation-table method discussed below.)

I will also need the periodic version of the $\mathbf{C}$ dyadic (or "MFIE kernel"),

$$\overline{\mathbf{C}}(\mathbf{x},\mathbf{x}') = \sum_{\mathbf{L}} e^{i\mathbf{k}_B\cdot\mathbf{L}} \mathbf{C}(\mathbf{x}-\mathbf{x}'-\mathbf{L})$$

with components

$$\begin{aligned}\overline{C}_{ij}(\mathbf{x},\mathbf{x}') &= \sum_{\mathbf{L}} e^{i\mathbf{k}_B\cdot\mathbf{L}} C_{ij}(\mathbf{x}-\mathbf{x}'-\mathbf{L}) \\ &= \frac{1}{ik}\epsilon_{ij\ell}\partial_\ell \sum_{\mathbf{L}} e^{i\mathbf{k}_B\cdot\mathbf{L}} G_0(\mathbf{x}-\mathbf{x}'-\mathbf{L}).\end{aligned}$$

Transpositional symmetries of periodic Green's functions The non-periodic $\mathbf{G}$ and $\mathbf{C}$ dyadics are invariant under simultaneous transposition of indices and inversion of argument:

$$G_{ij}(\mathbf{r}) = G_{ji}(-\mathbf{r}), \qquad C_{ij}(\mathbf{r}) = C_{ji}(-\mathbf{r}). \tag{68}$$

Now consider the implications of this for the periodic dyadics. In particular, we write

$$\overline{G}_{ij}(\mathbf{k}_B;\mathbf{x},\mathbf{x}') = \sum_{\mathbf{L}} e^{i\mathbf{k}_B\cdot\mathbf{L}} G_{ij}(\mathbf{x}-\mathbf{x}'-\mathbf{L})$$

Use (68):

$$= \sum_{\mathbf{L}} e^{i\mathbf{k}_B\cdot\mathbf{L}} G_{ji}(\mathbf{x}'-\mathbf{x}'+\mathbf{L})$$

Relabel the summation variable according to $\mathbf{L} \to -\mathbf{L}$:

$$\begin{aligned} &= \sum_{\mathbf{L}} e^{-i\mathbf{k}_{\rm B}\cdot\mathbf{L}} G_{ji}(\mathbf{x}' - \mathbf{x} - \mathbf{L}) \\ &= \overline{G}_{ji}(-\mathbf{k}_{\rm B}; \mathbf{x}', \mathbf{x}) \end{aligned} \tag{69a}$$

and similarly

$$\overline{C}_{ij}(\mathbf{k}_{\rm B}; \mathbf{x}, \mathbf{x}') = \overline{C}_{ji}(-\mathbf{k}_{\rm B}; \mathbf{x}', \mathbf{x}). \tag{69b}$$

Thus the periodic $\mathbf{G}$ and $\mathbf{C}$ dyadics are invariant under simultaneous transposition of indices, interchange of $\mathbf{x}, \mathbf{x}'$, and inversion of the Bloch vector.

Translational symmetries of periodic Green's functions Suppose the lattice basis vectors are $\mathbf{L}_1, \mathbf{L}_2$. Then we can write the sum that defines the scalar periodic Green's function in the form

$$\overline{G}_0(\mathbf{r}) = \sum_{n_1,n_2=-\infty}^{\infty} e^{i\mathbf{k}_{\rm B}\cdot(n_1\mathbf{L}_1 + n_2\mathbf{L}_2)} G_0(\mathbf{r} - n_1\mathbf{L}_1 - n_2\mathbf{L}_2)$$

Now consider evaluating $\overline{G}$ at an argument displaced through one full lattice basis vector:

$$\overline{\mathbf{G}}(\mathbf{r} + \mathbf{L}_1) = \sum_{n_1,n_2=-\infty}^{\infty} e^{i\mathbf{k}_{\rm B}\cdot(n_1\mathbf{L}_1 + n_2\mathbf{L}_2)} G_0(\mathbf{r} + \mathbf{L}_1 - n_1\mathbf{L}_1 - n_2\mathbf{L}_2)$$

Add and subtract $\mathbf{L}_1$ in the exponent of the Bloch factor:

$$= e^{i\mathbf{k}_{\rm B}\cdot\mathbf{L}_1} \sum_{n_1,n_2=-\infty}^{\infty} e^{i\mathbf{k}_{\rm B}\cdot[(n_1-1)\mathbf{L}_1 + n_2\mathbf{L}_2]} G_0(\mathbf{r} - (n_1-1)\mathbf{L}_1 - n_2\mathbf{L}_2)$$

Now just redefine $n_1 \to n_1 - 1$ in the infinite sum:

$$= e^{i\mathbf{k}_{\rm B}\cdot\mathbf{L}_1} \overline{\mathbf{G}}(\mathbf{r}).$$

More generally, for any lattice vector $\mathbf{L}$ I have

$$\overline{\mathbf{G}}(\mathbf{r} + \mathbf{L}) = e^{i\mathbf{k}_{\rm B}\cdot\mathbf{L}} \overline{\mathbf{G}}(\mathbf{r}).$$

16.3 Discretized EFIE formulation

Now consider solving for $\mathbf{K}(\mathbf{x})$ in the presence of illumination by an external Bloch-periodic field $\mathbf{E}^{\rm inc}$. We suppose that the current distribution in the unit cell is represented approximately by an expansion in basis functions $\{\mathbf{b}_\alpha(\mathbf{x})\}$:

$$\mathbf{K}(\mathbf{x}) \approx k_\alpha \mathbf{b}_\alpha(\mathbf{x}). \tag{70}$$

The electric-field integral equation reads

$$\mathbf{E}_{\parallel}^{\rm scat}(\mathbf{x}) = -\mathbf{E}_{\parallel}^{\rm inc}(\mathbf{x}). \tag{71}$$

As in the usual compact-surface case, inserting (67) and (70) and testing with each element in the set $\{\mathbf{b}_\alpha\}$ yields a discretized PBC EFIE:

$$\sum_\beta \underbrace{\left\langle \mathbf{b}_\alpha \middle| ikZ_0 \overline{\mathbf{G}} \middle| \mathbf{b}_\beta \right\rangle}_{\mathbf{M}_{\alpha\beta}} k_\beta = -\left\langle \mathbf{b}_\alpha \middle| \mathbf{E}^{\rm inc} \right\rangle \tag{72}$$

In other words, we obtain a formulation that looks exactly like the formulation for compact objects, with the only difference being that the elements of the BEM matrix involve the $\overline{\mathbf{G}}$ kernel in place of the usual $\mathbf{G}$ dyadic Green's function.

Note that the testing procedure that leads to (72) is only testing the satisfaction of equation (71) for points $\mathbf{x}$ *in the unit cell.* However, the Bloch-periodicity of the incident and scattered fields ensures that satisfaction of the equation throughout the unit cell implies its satisfaction everywhere.

16.4 Symmetries of the PBC BEM matrix

For a PEC structure, the α, β element of the BEM matrix is

$$\begin{aligned}
M_{\alpha\beta}(\mathbf{k}_{\rm B}) &= ik\left\langle \mathbf{b}_\alpha \middle| \overline{\mathbf{G}}(\mathbf{k}_{\rm B}) \middle| \mathbf{b}_\beta \right\rangle \\
&= ik \int \Big\{ b_{\alpha i}(\mathbf{x}_\alpha) \underbrace{\overline{G}_{ij}(\mathbf{k}_{\rm B};\mathbf{x}_\alpha,\mathbf{x}_\beta)}_{=\overline{G}_{ji}(-\mathbf{k}_{\rm B};\mathbf{x}_\beta,\mathbf{x}_\alpha)} b_{\beta j}(\mathbf{x}_\beta) \Big\} \, d\mathbf{x}_\alpha d\mathbf{x}_\beta \\
&= ik\left\langle \mathbf{b}_\beta \middle| \overline{\mathbf{G}}(-\mathbf{k}_{\rm B}) \middle| \mathbf{b}_\alpha \right\rangle \\
&= M_{\beta\alpha}(-\mathbf{k}_{\rm B})
\end{aligned}$$

where we used equation (69a). For a dielectric structure, the matrix elements also involve inner products with $\overline{\mathbf{C}}$ dyadics, but since $\overline{\mathbf{C}}$ satisfies the same symmetry as $\overline{\mathbf{G}}$ (**??**b), a similar equation holds in that case.

Thus in general for both PEC and non-PEC BEM matrices we have

$$\mathbf{M}(\mathbf{k}_{\rm B}) = \Big[\mathbf{M}(-\mathbf{k}_{\rm B})\Big]^T \tag{73}$$

where T denotes the *non-conjugate* transpose.

Symmetries in the imaginary frequency case

For equilibrium Casimir computations we need elements of the BEM matrix at imaginary frequencies.

$$\mathbf{M}(i\xi, \mathbf{k}_{\rm B}) = \mathbf{M}(i\xi, \mathbf{k}_{\rm B})^\dagger$$

17 PBC geometries in SCUFF-EM

17.1 Overview

LIBSCUFF supports Bloch-periodic boundary conditions for periodically repeated geometries. In this case,

- The `.scuffgeo` file will contain a `LATTICE...ENDLATTICE` section defining between one and three lattice basis vectors $\mathbf{L}_1, \mathbf{L}_2, \mathbf{L}_3$. (In the present discussion we will consider the common case of two-dimensional periodicity, so we have two lattice basis vectors $\mathbf{L}_1, \mathbf{L}_2$.) We assume that $\mathbf{L}_1, \mathbf{L}_2$ have no component in the z direction.
- The only portion of the geometry that is meshed is that contained with the "unit cell."
- We will refer to the lattice cell obtained by displacing the unit cell through displacement vector $\mathbf{L} = n_1\mathbf{L}_1 + n_y\mathbf{L}_2$ as "lattice cell (n_1, n_2)" or sometimes "lattice cell $\mathbf{L}$".
- All currents and fields in lattice cell (n_1, n_2) are understood to be equal to the corresponding currents and fields in lattice cell $(0, 0)$ times a Bloch phase factor $e^{i\mathbf{k}_B\cdot\mathbf{L}}$ where $\mathbf{k}_B$ is the Bloch wavevector.

17.2 Straddlers

Suppose we are trying to mesh the unit cell of a square-lattice geometry. Consider the square mesh shown in the upper portion of Figure 8. If LIBSCUFF were given this mesh as a description of a *compact* surface, it would assign a total of 40 basis functions, as indicated by the arrows in the lower portion of Figure 8. In particular, no basis functions would be assigned to exterior edges. Such a set of basis functions would have the property that, when we consider the infinite surface obtained by periodically replicating the mesh and the basis functions, no currents could flow from one unit cell to the next; all currents would be localized within the area of individual unit cells. To remedy this difficulty, LIBSCUFF automatically adds *straddlers* to the surface meshes specified to the code in geometries involving extended surfaces. This is illustrated in Figure 9.

17.3 Evaluation of surface currents within the unit cell

When evaluating the $\mathbf{K}$ and $\mathbf{N}$ surface-current distributions at panels that border the upper or right edges of the unit-cell mesh, we have to be careful to account for the contribution of straddlers.

For example, consider evaluating the electric surface current at oints $\mathbf{x}$ inside panel $\mathcal{P}_{24}$ in Figure 9. There are three RWG basis functions that contribute to the current at this point: the functions associated with edges 29 and 42, and the periodic image of the function associated with edge 40. Thus we compute

$$\mathbf{K}(\mathbf{x}) = k_{29}\mathbf{b}_{29}(\mathbf{x}) + k_{42}\mathbf{b}_{42}(\mathbf{x}) + e^{i\mathbf{k}_B\cdot\mathbf{L}_1}k_{40}\mathbf{b}_{40}(\mathbf{x}-\mathbf{L}_1)$$

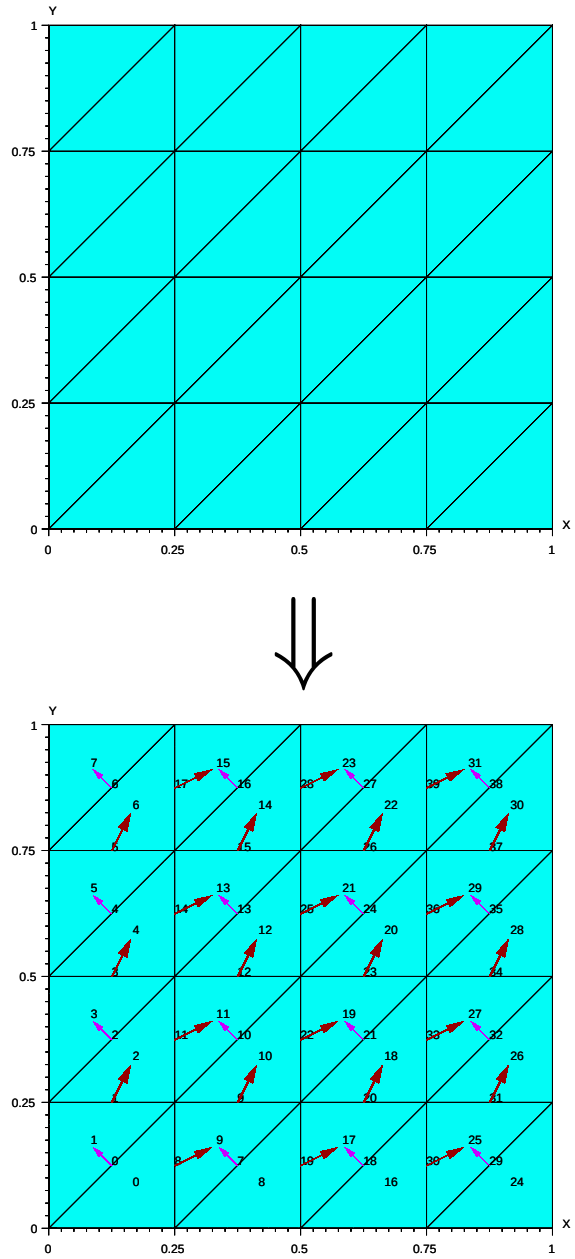

Figure 8: The usual assignment of RWG basis functions to an input surface mesh. Integers inside panels denote panel indices. Indices lying atop edges denote RWG basis-function indices. Arrows indicate directions of current flow.

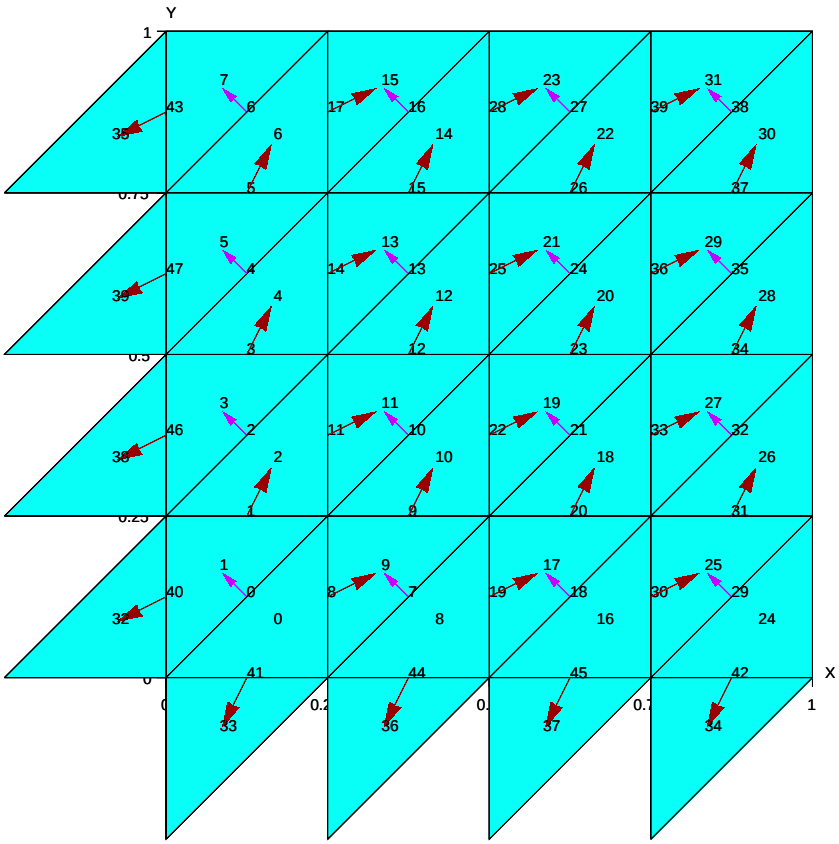

Figure 9: Straddlers. Integers inside panels denote panel indices. Indices lying atop edges denote RWG basis-function indices. Arrows indicate directions of current flow.

where $\mathbf{L}_1$ is the lattice basis vector through which we translate points in panel 32 to yield points in panel 24. [In this case we have $\mathbf{L}_1 = (1, 0)$.]

17.4 Relations between BEM matrix elements

Looking at Figure 9, it seems obvious that BEM matrix elements between the pair of basis functions $\{\mathbf{b}_2, \mathbf{b}_{24}\}$ will be identical to those between the pair $\{\mathbf{b}_4, \mathbf{b}_{27}\}$. (This much would be true even if we *weren't* talking about periodic geometries.)

Slightly less obvious is that matrix elements between the pair $\{\mathbf{b}_6, \mathbf{b}_{18}\}$ will *also* be related to matrix elements between the above two pairs—in fact, the elements will be *identical* for $\mathbf{k}_B = 0$ and will differ by only a phase factor for $\mathbf{k}_B \neq 0$. Let's now derive this relationship.

Let $\mathbf{L}$ be a lattice vector and let $\{\mathbf{b}_\alpha, \mathbf{b}_\beta\}$ and $\{\mathbf{b}_{\alpha'}, \mathbf{b}_{\beta'}\}$ be two pairs of RWG basis functions for which the displacement between centroids differs by $\mathbf{L}$. That is, we have

$$\mathbf{x}_{0\beta} - \mathbf{x}_{0\alpha} = \mathbf{x}_{0\beta'} - \mathbf{x}_{0\alpha'} + \mathbf{L}$$

where e.g. $\mathbf{x}_{0\beta}$ denotes the centroid of the support of $\mathbf{b}_\beta$. Examples of basis-function pairs in the mesh of Figure 9 for which this condition is satisfied include

$$\begin{array}{lllllllll} (\alpha,\beta) & = & (4,27), & (\alpha',\beta') & = & (6,18), & \mathbf{L} & = & (0,1) \\ (\alpha,\beta) & = & (0,32), & (\alpha',\beta') & = & (7,2), & \mathbf{L} & = & (1,0). \end{array}$$

17.5 Assembly of BEM matrix blocks

For a geometry in which the unit cell contains N surfaces, the BEM matrix at Bloch wavevector $\mathbf{k}_B$ has the structure

$$\mathbf{M}(\mathbf{k}_B) = \begin{pmatrix} \mathbf{T}_1(\mathbf{k}_B) & \mathbf{U}_{12}(\mathbf{k}_B) & \cdots & \mathbf{U}_{1N}(\mathbf{k}_B) \\ \mathbf{U}_{21}(\mathbf{k}_B) & \mathbf{T}_2(\mathbf{k}_B) & \cdots & \mathbf{U}_{2N}(\mathbf{k}_B) \\ \vdots & \vdots & \ddots & \vdots \\ \mathbf{U}_{N1}(\mathbf{k}_B) & \mathbf{U}_{N2}(\mathbf{k}_B) & \cdots & \mathbf{T}_N(\mathbf{k}_B) \end{pmatrix} \tag{74}$$

where $\mathbf{U}_{mn}$ describes the interaction of surfaces m and n and $\mathbf{T}_m$ describes the self-interaction of surface m.

Off-diagonal blocks

The off-diagonal blocks have the structure

$$\begin{aligned}\mathbf{U}_{mn}(\mathbf{k}_{\rm B}) =& \mathbf{U}^{00}_{mn} \\ &+ e^{i\mathbf{k}_{\rm B}\cdot\mathbf{L}_1}\mathbf{U}^{+0}_{mn} + e^{-i\mathbf{k}_{\rm B}\cdot\mathbf{L}_1}\mathbf{U}^{-0}_{mn} \\ &+ e^{i\mathbf{k}_{\rm B}\cdot\mathbf{L}_2}\mathbf{U}^{0+}_{mn} + e^{-i\mathbf{k}_{\rm B}\cdot\mathbf{L}_2}\mathbf{U}^{0-}_{mn} \\ &+ e^{i\mathbf{k}_{\rm B}\cdot(\mathbf{L}_1+\mathbf{L}_2)}\mathbf{U}^{++}_{mn} + e^{-i\mathbf{k}_{\rm B}\cdot(\mathbf{L}_1+\mathbf{L}_2)}\mathbf{U}^{--}_{mn} \\ &+ e^{i\mathbf{k}_{\rm B}\cdot(\mathbf{L}_1-\mathbf{L}_2)}\mathbf{U}^{+-}_{mn} + e^{-i\mathbf{k}_{\rm B}\cdot(\mathbf{L}_1-\mathbf{L}_2)}\mathbf{U}^{-+}_{mn} \\ &+ \mathbf{U}^{\rm AB9}_{mn}(\mathbf{k}_{\rm B}).\end{aligned} \tag{75}$$

In this equation, $\mathbf{U}^{\sigma\sigma'}_{mn}$ is the usual (non-periodic) matrix describing the interaction of surface m with a *displaced* copy of surface n; the displacement is through displacement vector $\sigma\mathbf{L}_1 + \sigma'\mathbf{L}_2$ where $\sigma, \sigma' \in \{-1, 0, 1\}$. On the other hand, $\mathbf{U}^{\rm AB9}_{mn}$ represents the interaction of surface m with the infinite set of Bloch-phased and displaced copies of surface n *excluding* the contribution of the innermost 9 grid cells ("AB9" stands for "all but 9.")

The point of the decomposition (75) is that the matrix blocks $\mathbf{U}^{\sigma\sigma'}_{mn}$ are *independent of* $\mathbf{k}_B$ and hence need only be computed once at a given angular frequency, after which they may be reused for any number of calculations at different points in the Brillouin zone.

In SCUFF-EM, the $\mathbf{k}_{\rm B}$-independent matrix blocks $\mathbf{U}^{\sigma\sigma'}_{mn}$ are computed using the ordinary algorithm for assembling the blocks of the BEM matrix for compact (non-periodic) geometries. An advantage of this is that singular integrals involving pairs of panels in adjacent cells with common edges or vertices are handled correctly using singular-integral evaluation techniques present in SCUFF-EM. For example, in the mesh of Figure 9, panel 1 of the unit-cell mesh has a common edge with panel 24 of the $(-1, 0)$ mesh image.

Transposes of off-diagonal blocks

Once we have computed the $\mathbf{U}^{\sigma\sigma'}_{mn}$ blocks for the mn block of the BEM, we may re-use them to compute the nm block, as follows based on equation (73):

$$\mathbf{U}_{nm}(\mathbf{k}_{\rm B}) = \Big[\mathbf{U}_{mn}(-\mathbf{k}_{\rm B})\Big]^T \tag{76}$$

$$\begin{aligned}=& \Big[\mathbf{U}^{00}_{mn}]^T \\ &+ e^{-i\mathbf{k}_{\rm B}\cdot\mathbf{L}_1}\Big[\mathbf{U}^{+0}_{mn}\Big]^T + e^{i\mathbf{k}_{\rm B}\cdot\mathbf{L}_1}\Big[\mathbf{U}^{-0}_{mn}\Big]^T \\ &+ e^{-i\mathbf{k}_{\rm B}\cdot\mathbf{L}_2}\Big[\mathbf{U}^{0+}_{mn}\Big]^T + e^{+i\mathbf{k}_{\rm B}\cdot\mathbf{L}_2}\Big[\mathbf{U}^{0-}_{mn}\Big]^T \\ &+ e^{-i\mathbf{k}_{\rm B}\cdot(\mathbf{L}_1+\mathbf{L}_2)}\Big[\mathbf{U}^{++}_{mn}\Big]^T + e^{+i\mathbf{k}_{\rm B}\cdot(\mathbf{L}_1+\mathbf{L}_2)}\Big[\mathbf{U}^{--}_{mn}\Big]^T \\ &+ e^{-i\mathbf{k}_{\rm B}\cdot(\mathbf{L}_1-\mathbf{L}_2)}\Big[\mathbf{U}^{+-}_{mn}\Big]^T + e^{+i\mathbf{k}_{\rm B}\cdot(\mathbf{L}_1-\mathbf{L}_2)}\Big[\mathbf{U}^{-+}_{mn}\Big]^T \\ &+ \mathbf{U}^{\rm AB9}_{nm}(\mathbf{k}_{\rm B}).\end{aligned} \tag{77}$$

Diagonal blocks

For the diagonal blocks there are additional symmetries, e.g. $\mathbf{T}_m^{--} = \left[\mathbf{T}_m^{++}\right]^T$, and hence the equivalent of (75) reads

$$\begin{aligned}\mathbf{T}_m(\mathbf{k}_\mathrm{B}) =& \mathbf{T}_m^{00} \\ &+ e^{i\mathbf{k}_\mathrm{B}\cdot\mathbf{L}_1}\mathbf{T}_m^{+0} + e^{-i\mathbf{k}_\mathrm{B}\cdot\mathbf{L}_1}\left[\mathbf{T}_m^{+0}\right]^T \\ &+ e^{i\mathbf{k}_\mathrm{B}\cdot\mathbf{L}_2}\mathbf{T}_m^{0+} + e^{-i\mathbf{k}_\mathrm{B}\cdot\mathbf{L}_2}\left[\mathbf{T}_m^{0+}\right]^T \\ &+ e^{i\mathbf{k}_\mathrm{B}\cdot(\mathbf{L}_1+\mathbf{L}_2)}\mathbf{T}_m^{++} + e^{-i\mathbf{k}_\mathrm{B}\cdot(\mathbf{L}_1+\mathbf{L}_2)}\left[\mathbf{T}_m^{++}\right]^T \\ &+ e^{i\mathbf{k}_\mathrm{B}\cdot(\mathbf{L}_1-\mathbf{L}_2)}\mathbf{T}_m^{+-} + e^{-i\mathbf{k}_\mathrm{B}\cdot(\mathbf{L}_1-\mathbf{L}_2)}\left[\mathbf{T}_m^{+-}\right]^T \\ &+ \mathbf{T}_m^{\mathrm{AB9}}(\mathbf{k}_\mathrm{B}).\end{aligned} \tag{78}$$

Hence to assemble $\mathbf{T}(\mathbf{k}_\mathrm{B})$ we need only compute and store 5 $\mathbf{k}_\mathrm{B}$-independent blocks $\mathbf{T}^{\sigma\sigma'}$ instead of the 9 $\mathbf{k}_\mathrm{B}$-independent blocks required to assemble $\mathbf{U}(\mathbf{k}_\mathrm{B})$.

Assessing the connectivity of regions

An important subtlety in the BEM matrix assembly for dielectric geometries treated by the PMCHWT formulation concerns the question of the "extendedness" or connectivity of material regions.

In general, the surfaces m, n whose interaction is described by the $\mathbf{T}_m$ and $\mathbf{U}_{mn}$ blocks in (74) will interact through one or two common *regions* (material media). (More specifically, $\mathbf{T}$ blocks will typically involve two common regions, while $\mathbf{U}$ blocks will typically involve one common region.)

The BEM matrix elements

$$I_n\Big[g(r)\Big] \equiv \int_0^1 w^n g(wr) dw$$

1. First, for $g(r) = r^p$ we have simply $I_n\big[g(r)\big] = \frac{r^p}{p+n+1}$.

2. Next, for the case $g(r) = \frac{e^{ikr}}{r}$ we find

$$I_n\Big[g(r)\Big] = \frac{1}{nrT_n}\Big[1 - e^{ikr}\Big(T_0 + T_1 + \cdots + T_{n-1}\Big)\Big].$$

   where $T_n \equiv \frac{(-ikr)^n}{n!}$. For computational purposes, this expression ... $|kr| > 0.1$ ...

$$\begin{aligned} I_n\Big[g(r)\Big] = &= \frac{e^{ikr}}{nrT_n}\Big[e^{-ikr} - T_0 - T_1 - \cdots - T_{n-1}\Big] \\ &= \frac{e^{ikr}}{nr} \cdot \texttt{ExpRel}_n(-ikr) \end{aligned}$$

$$\begin{aligned} \texttt{ExpRel}_n(-ikr) &\equiv \frac{1}{T_n}\Big[e^{-ikr} - T_0 - T_1 - \cdots - T_{n-1}\Big] \\ &= 1 + \frac{(-ikr)}{(n+1)} + \frac{(-ikr)^2}{(n+1)(n+2)} + \cdots \quad = n! \sum_{m=0}^{\infty} \frac{(-ikr)^m}{(m+n)!} \end{aligned}$$

3. Finally, for the case $g(r) = \frac{(ikr-1)e^{ikr}}{r^3}$, we have

$$I_n\Big[g(r)\Big] = \frac{n-1}{(n-2)T_{n-2}r^3}\Big[1 - e^{ikr}\Big(T_0 + T_1 + \cdots + T_{n-3} + \frac{n-2}{n-1}T_{n-2}\Big)\Big].$$

   For small kr we again rewrite this in the form

$$I_n\Big[g(r)\Big] = \frac{(n-1)e^{ikr}}{(n-2)T_{n-2}r^3}\Big[e^{-ikr} - T_0 - T_0 - \cdots - T_{n-2} - \frac{1}{n-1}T_{n-2}\Big]$$

   where again $T_n \equiv \frac{(-ikr)^n}{n!}$.